Low-temperature properties of a model glass. II. Specific heat and thermal transport

Eric R. Grannan*
Laboratory of Atomic and Solid State Physics, Cornell University, Ithaca, New York 14853-2501

Mohit Randeria†
Department of Physics, University of Illinois at Urbana-Champaign, 1110 West Green Street, Urbana, Illinois 61801 and Materials Research Laboratory, University of Illinois at Urbana-Champaign, 104 South Goodwin Avenue, Urbana, Illinois 61801

James P. Sethna
Laboratory of Atomic and Solid State Physics, Cornell University, Ithaca, New York 14853-2501
(Received 5 May 1989; revised manuscript received 20 October 1989)

We study the low-temperature properties of glasses using the elastic dipole model introduced in the preceding paper (I). We show that harmonic excitations about the frozen ground states of the defect Hamiltonian dominate thermal properties in the 1–10-K regime. We numerically determine the density of states for the defect modes from the simulation of I. The coupling of long-wavelength phonons to the defect modes is treated within perturbation theory, and is shown to lead to frequency-dependent softening of the medium and to strong phonon scattering in the terahertz frequency region. The defect modes account for the excess specific heat seen as the bump in C/T^3. Resonant scattering of acoustic phonons off the defect modes leads to the plateau in the thermal conductivity. We compare our results with experiments on the orientational glass KBr:KCN and on vitreous silica.

I. INTRODUCTION

The universal low-temperature properties[1,2] of amorphous materials have been a subject of considerable interest for a long time. The very-low-temperature ($T<1$ K) behavior was understood within the phenomenological two-level system[3] (TLS) framework of Anderson, Halperin, Varma, and Phillips shortly after the first experimental observations.[4] However, universal properties like the plateau in the thermal conductivity and the excess specific heat between 1 and 10 K have long resisted even a qualitative explanation.

It is only very recently that progress has been made on these universal "intermediate"-temperature properties. This progress has come from two rather different directions. First, experiments[5] on disordered alkali-halide–alkali-cyanide crystals which showed all of the universal low-temperature properties of glasses led to a detailed quantitative analysis[6,7] of these features in a model orientational glass by the authors. Our analysis revealed the existence of additional harmonic excitations in the tetrahertz frequency regime, which resonantly scatter the phonons to produce the plateau. Ideas similar to ours, but considerably different in detail, have been independently proposed by other authors.[8,9] Second, in a parallel development, inelastic-neutron-scattering experiments[10] on vitreous silica gave direct evidence for localized harmonic excitations, in addition to phonons, in the terahertz frequency range. While a straightforward connection could be made[10] between these modes and the excess specific heat, the evidence relating these to the thermal-conductivity plateau in structural glasses has been only circumstantial so far.

In this paper we study the intermediate-temperature properties of glasses within the context of the elastic dipole model of I (Ref. 11). While this model was originally formulated[6] for a particular orientational glass, in Sec. II of I we have given arguments to espouse it as one of the simplest phenomenological models for studying the low-temperature properties of all glasses. Here we will apply our model to describe the intermediate-temperature properties for both orientational glasses and vitreous silica.

Let us begin by briefly summarizing the main ideas of I. There we introduced a model of elastic dipole defects embedded at random locations in an elastic continuum, with the defects acting as local sources of stress. The defects and the phonons—the harmonic excitations of the elastic medium—form a strongly interacting random system, and in order to proceed we made certain simplifying assumptions. We used elasticity theory to obtain the strain-mediated interaction between defects, making the approximation that the phonons mediate essentially instantaneous interactions. This led to an anisotropic, $1/r^3$ Hamiltonian which describes the interacting defect dipoles. We then performed a Monte Carlo simulation of the defect Hamiltonian, and studied the glassy ground states and certain excitations involving dipolar reorientation; see I (Ref. 11) for details.

In this paper we shall study the *harmonic excitations* about the disordered ground states obtained in I. We show that the interaction of the phonons with these "additional" harmonic excitations of the defect system is responsible for the intermediate-temperature universal properties of glasses.

In Sec. II of the present paper we introduce the *libration modes*, which are the normal modes of the small angular oscillations of the dipoles about their frozen orientations. We show that the density of states (DOS) for the libration modes is a strongly peaked function of frequency. After identifying the important harmonic excitations about the disordered ground states, we analyze the coupling of these modes with the phonons and its effects on the elastic and thermal properties of the system in the rest of this paper.

We begin in Sec. III by studying the response of the system to a static external strain field. We show that the relaxation of the defects leads to a softening of the shear response of the material, although the bulk modulus is unchanged. This is in excellent agreement with elastic data for $(KBr)_{1-x}(KCN)_x$ as a function of the cyanide concentration x.

We next study, in Sec. IV, the elastic response of the system to a finite-frequency external perturbation. In addition to a frequency-dependent in-phase response, we also find an absorptive part with strong frequency dependence. The latter represents resonant scattering of phonons from the libration modes.

In Sec. V we discuss the *total* density of harmonic excitations. We show the need to include the coupling of the phonons and the defect libration modes in determining this DOS. We derive results for the specific heat and show that the libration modes will give rise to the bump in C/T^3, which is a universal feature of all glasses.

We focus on thermal transport in Sec. VI. We begin with a brief review of various other phonon-scattering mechanisms in glasses, which together fail to explain the thermal-conductivity plateau. We then discuss the importance of resonant scattering from librations for thermal transport in the 1–10-K temperature range. We discuss how this strong resonant scattering, together with the temperature-independent scattering of low-energy phonons, leads to a plateau in the thermal conductivity.

We next compare the predictions of our theory in Sec. VII with thermal-conductivity and specific-heat experiments: first with the orientational glass KBr:KCN, and then with vitreous silica. For the former we have a microscopic identification of the libration modes with the angular oscillations of the cyanide molecules. The fits to the experiment are therefore without any free parameter in KBr:KCN. On the other hand, for vitreous silica, the elastic dipole model has no microscopic interpretation. The two parameters of the model are obtained from fitting the total density of harmonic excitations in the model to that measured[10] by inelastic-neutron-scattering experiments on a-SiO_2. This determines the thermal-conductivity plateau and excess specific heat without any additional free parameters.

In Sec. VIII we discuss the universality of the plateau within our model, and also discuss the extent to which our model is successful in describing arbitrary glasses.

Section IX contains a critical discussion of the various approximations we have made in the analysis presented in this paper and its companion (I), together with a discussion of the strengths and weaknesses of our approach.

We describe other approaches which have been proposed to understand the universal low-temperature properties of glasses in Sec. X, and contrast these with the elastic dipole model analyzed in this paper. Finally, Sec. XI contains our conclusions.

In the Appendix we show how to go from the "computer" units used in the simulation of the defect system to physical numbers.

II. NORMAL MODES

In this paper we discuss two types of harmonic excitations. First, there are the phonon modes[12] of the elastic medium which both mediate the interactions between the defects and also contribute to thermal transport. Second, there are the harmonic excitations of the dipole degrees of freedom about their metastable ground state. These two types of excitations are coupled linearly, and thus, in principle, we ought to be studying the true normal modes of the coupled system, e.g., by diagonalizing the random harmonic system. We make the conceptual separation between phonon and defect modes for two reasons. First, our simulation of the random defect system is necessarily much smaller than the phonon wavelengths relevant for low-temperature thermal transport. Second, there is a separation of frequency scales which allows us to incorporate the bulk of the phonon modes, i.e., those near the Debye frequency, into the effective interaction between defects. The coupling of the long-wavelength phonons to the defect modes is then treated perturbatively.

In this section we introduce the libration modes, which are the harmonic excitations of the defect subsystem. In I we simulated a system of elastic dipoles $Q_{ij} = Q_0(\hat{n}_i\hat{n}_j - \frac{1}{3}\delta_{ij})$, placed randomly on the sites $\mathbf{x}$ of a fcc lattice. The dipoles interact via the Hamiltonian

$$H = -\tfrac{1}{2} \sum_{\substack{\mathbf{x},\mathbf{x}' \\ (\mathbf{x}\neq\mathbf{x}')}} Q_{ij}(\mathbf{x}')J_{ijkl}(\mathbf{x}-\mathbf{x}')Q_{kl}(\mathbf{x}') \ , \tag{1}$$

where J_{ijkl} is the real-space Green function for the strain of a dipole in an isotropic elastic medium. In I we numerically found ground states of this system, where the dipoles are frozen in random orientations $\hat{\mathbf{n}}(\mathbf{x}) = (\sin\theta_{\mathbf{x}}\cos\phi_{\mathbf{x}}, \sin\theta_{\mathbf{x}}\sin\phi_{\mathbf{x}}, \cos\theta_{\mathbf{x}})$.

Since the ground states we find in the simulation are local minima of the energy, the energy for small deviations from a ground state is given by a quadratic form. Each dipole has two angular degrees of freedom; we will write the angular coordinates of the dipole at site $\mathbf{x}$ as $\xi_{\mathbf{x}1}$ and $\xi_{\mathbf{x}2}$. These could, for example, be given by small deviations from the frozen orientation $\hat{\mathbf{n}}$ of the dipole, so that $\delta\xi_{\mathbf{x}1} = \delta\theta_{\mathbf{x}}$ and $\delta\xi_{\mathbf{x}2} = \sin\theta_{\mathbf{x}}\delta\phi_{\mathbf{x}}$. We can then write the potential energy as

$$H_{\text{int}} = E_0 + \tfrac{1}{2} \sum_{\mathbf{x},\alpha;\mathbf{y},\beta} D_{\mathbf{x}\alpha,\mathbf{y}\beta}\delta\xi_{\mathbf{x}\alpha}\delta\xi_{\mathbf{y}\beta} + \cdots \ . \tag{2}$$

The dynamical matrix D above is defined as

$$D_{\mathbf{x}\alpha,\mathbf{y}\beta} \equiv \frac{\partial^2 H_{\text{int}}}{\partial\xi_{\mathbf{x}\alpha}\partial\xi_{\mathbf{y}\beta}} \ , \tag{3}$$

where the derivatives are evaluated at the frozen ground-

state orientations.

We can diagonalize the dynamical matrix to determine the normal modes of the defect system, which we call "libration modes," since these are the small angular oscillations of the defect dipoles about their frozen orientations. We will show below that these modes are very important for the intermediate-temperature properties of our model.

Let us define $M_{b,\mathbf{x}\alpha}$ to be the orthogonal matrix that diagonalizes the dynamical matrix D, so that

$$M_{b,\mathbf{x}\alpha}D_{\mathbf{x}\alpha,\mathbf{y}\beta}M_{b',\mathbf{y}\beta}=I\Omega_b^2\delta_{b,b'} . \tag{4}$$

Here, I is the moment of inertia of a defect and Ω_b is the oscillation frequency of the bth normal mode; $b=1,2,\ldots,2N$ in a system with N defect dipoles. The corresponding eigenvector of the dynamical matrix is

$$\psi_b=\sum_{\mathbf{x}}\sum_{\alpha=1}^{2} M_{b,\mathbf{x}\alpha}\xi_{\mathbf{x}\alpha} . \tag{5}$$

$M_{b,\mathbf{x}\alpha}$ is thus the amplitude of the angular coordinate $\xi_{\mathbf{x}\alpha}$ in the bth libration mode. We should emphasize that the eigenvectors of the dynamical matrix of a random system are not expected to be plane waves, which is indeed what we shall find.

The density of states (DOS) of the libration modes plays a major role in the subsequent analysis. We have obtained this DOS by diagonalizing the dynamical matrix for a particular frozen configuration and then averaging over approximately 10–20 different configurations. The density of states of the librations per unit volume, $p(\Omega)$, is plotted in Fig. 1. We have found that it is remarkably independent of the system size. For very small systems, say with a few defects, the DOS has sharp structure, but even for a $3\times3\times3$ lattice this structure is washed out and a single peak is obtained.

This peak in the libration DOS is very crudely related to the bare-barrier-height distribution $P(V)$ of I, Sec. VI, as follows. Each dipole "sits" in a local potential with a double-well structure, and a barrier height V to 180° reorientation which has a peaked distribution $P(V)$. If we make the gross simplification of assuming that each dipole is an independent Einstein oscillator, we obtain[7] a peaked DOS of small oscillations from the peaked distribution $P(V)$. (This crude "single-particle" estimate is only qualitatively correct, and is unable to fit both the plateau and the excess specific heat simultaneously, as discussed in Ref. 7.) The true defect normal modes obtained from the computer simulation are much more complicated than individual Einstein oscillators and are coupled oscillations of the dipoles about their frozen orientations. We have checked the degree of anharmonicity of these modes, and find that the deviation from harmonic behavior is less than 1% for temperatures below 20 K.

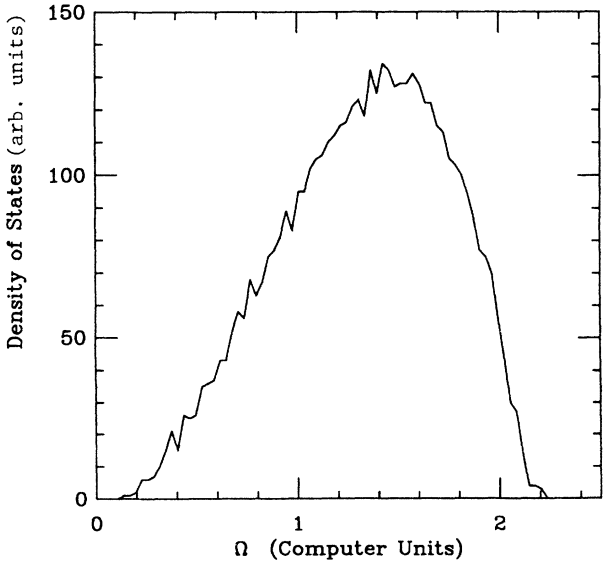

FIG. 1. Density of states $p(\Omega)$ for the defect libration modes from simulation with a defect concentration $x=0.5$. The frequency is in computer units.

A question of some importance is the nature of these eigenstates: are these modes localized or extended? We estimate the number of dipoles in a given mode using the participation ratio,

$$X_b=\frac{1}{N}\left[\sum_{\mathbf{x}}(M_{b,\mathbf{x}1}^2+M_{b,\mathbf{x}2}^2)^2\right]^{-1} . \tag{6}$$

We have defined this to normalize to the number of dipoles, so that a mode that is evenly distributed over all the dipoles will have a participation ratio of 1 and a localized mode will have $X_b\sim O(N^{-1})$. We find that both the very-high-frequency and very-low-frequency modes are localized; the modes at these frequencies have small participation ratios which do not depend on the system size. Figure 2 shows the participation (NX_b) as a function of frequency for various-size lattices at a concentration of

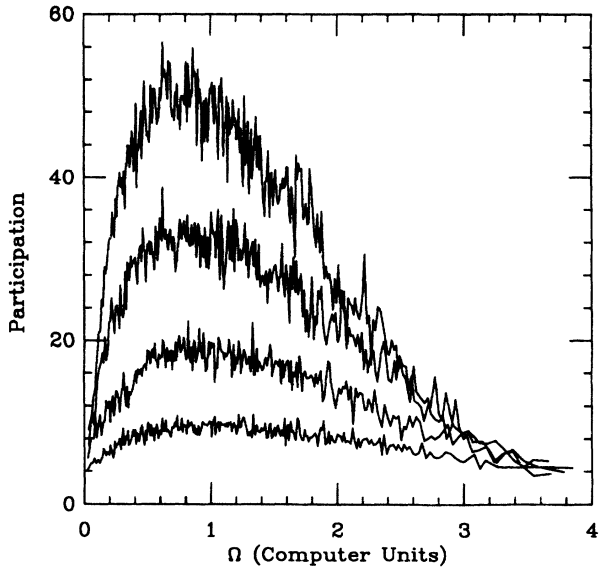

FIG. 2. Smoothed participation values for $x=0.25$, on lattices of length $L=3$, 4, 5, and 6. We plot $\langle N\rangle=4xL^3$ times the participation ratio because it is easier to see. Each point on the graph is the average of 20 points. The participation ratio is shrinking (slowly) with system size, but it is not clear whether it is going to zero as the system size goes to infinity. The peak of the participation *ratio* X_b (see text) for the four sizes is 0.33, 0.30, 0.26, and 0.23.

$x=0.25$, and we see that the participation ratio at intermediate frequencies is still increasing as we increase system size.

Thus, due to the extreme sensitivity of the participation ratio to finite-size effects, we cannot determine from our simulation if the modes in the center of the libration band are localized or extended. Even if they are extended, it is likely that energy diffusion via the librations is small; however, we have not addressed this question quantitatively. In the following we will simply assume that the libration modes do not contribute to thermal transport.

III. STATIC RESPONSE

The libration modes have two main effects on the phonons. The first is that they act to change the elastic constants of the medium. This is because the dipoles can adjust to take up stress in the material. The second main effect is to scatter phonons resonantly. We can determine these effects in a unified way by calculating a complex frequency-dependent susceptibility of the libration modes to the phonon strain fields. It is useful to first do a simpler calculation of the response of the dipoles to an externally applied *static* stress. This calculation is more physically transparent and serves to set the stage for the full frequency-dependent response.

Imagine applying an external stress to the medium. The Hamiltonian for the defect system coupled to an external stress σ^E_{ij} is given by[13]

$$H=-\tfrac{1}{2}\sum_{\substack{\mathbf{x},\mathbf{x}'\\(\mathbf{x}\neq\mathbf{x}')}} Q_{ij}(\mathbf{x}')J_{ijkl}(\mathbf{x}-\mathbf{x}')Q_{kl}(\mathbf{x}')-e^E_{ij}Q^I_{ij}-\frac{V}{2}e^E_{ij}\sigma^E_{ij}\ , \tag{7}$$

where $Q^I_{ij}=\sum_{\mathbf{x}}Q_{ij}(\mathbf{x})$ is the total (internal) dipole moment, and the "external" strain $e^E_{ij}=s_{ijkl}\sigma^E_{kl}$. Note that the $e^E_{ij}\sigma^E_{ij}$ contribution comes in with a *negative* sign in the total energy, since it involves both the (positive) elastic energy of the medium and the (negative) $p\,dV$ work done on the system.

We want to calculate the renormalization of the elastic constants due to the presence of the defects. The elastic constants give the linear response of an elastic medium, and for small external stresses we can make a harmonic approximation (2) for the defect Hamiltonian. Using (4), the first term of (7) is diagonalized to the form $\sum_b \frac{1}{2}I\Omega_b^2\psi_b^2$. We next linearize the second term of (7) in the dipole coordinates $\xi_{\mathbf{x}\alpha}$, and express is in terms of the normal modes, using the inverse of (5) given by $\xi_{\mathbf{x}\alpha}=\sum_b M_{b,\mathbf{x}\alpha}\psi_b$. Using

$$\delta Q_{ij}(\mathbf{x})=\sum_{b=1}^{2N}\sum_{\alpha=1}^{2}\frac{\partial Q_{ij}}{\partial\xi_{\mathbf{x}\alpha}}M_{b,\mathbf{x}\alpha}\psi_b\ , \tag{8}$$

the coupling between the libration modes and the external strain field can be written as $e^E_{ij}\sum_b C_{b,ij}\psi_b$, where we have defined a coupling constant

$$C_{b,ij}\equiv\sum_{\mathbf{x},\alpha}M_{b,\mathbf{x}\alpha}\frac{\partial Q_{ij}(\mathbf{x})}{\partial\xi_{\mathbf{x}\alpha}} \tag{9}$$

for each libration mode. Collecting these terms, the total energy of the system for small amplitudes in the normal modes is given by

$$H=E_0+\sum_b\tfrac{1}{2}I\Omega_b^2\psi_b^2-e^E_{ij}\sum_b C_{b,ij}\psi_b-\frac{V}{2}s_{ijkl}\sigma^E_{ij}\sigma^E_{kl}\ . \tag{10}$$

If we apply a static external stress field, the dipoles will just relax to their minimum-energy positions. Minimizing (10) with respect to ψ_b gives

$$\psi_b=\frac{e^E_{ij}C_{b,ij}}{I\Omega_b^2}=\frac{s_{ijkl}\sigma^E_{kl}C_{b,ij}}{I\Omega_b^2}\ , \tag{11}$$

and then the uniform strain field induced by the response of the dipoles to the external stress field is given by

$$\varepsilon_{mn}=\frac{1}{V}s_{klmn}\sum_b C_{b,kl}\frac{e^E_{ij}C_{b,ij}}{I\Omega_b^2}\ . \tag{12}$$

The "renormalized" compliance tensor[14] is then given by

$$s_{mnop}(\omega=0)=s_{mnop}+s_{klmn}s_{ijop}\frac{1}{V}\sum_b\frac{C_{b,ij}C_{b,kl}}{I\Omega_b^2}\ . \tag{13}$$

This result may also be obtained by substituting (11) back into (10), and identifying the renormalized compliance tensor as the coefficient of the term quadratic in the stress fields.

We use the notation $s_{mnop}(\omega)$ to determine the response at frequency ω. Throughout this paper, elastic and compliance constants without an argument are taken to be the (high-frequency) "bare" values. Before turning to the physics of this renormalization, we simplify our results by doing a spherical average.

A. Spherical average

We now want to spherically average the response to an external stress for several reasons. First, while we have already spherically symmetrized the bare elastic constants by starting with an isotropic medium, we place the defects randomly on the sites of a fcc lattice. This introduces a (average) cubic symmetry in our simulation. We will find that it greatly simplifies the later calculations, e.g., of thermal transport, to work with a spherical average. Second, the libration modes are obtained from a numerical simulation, and are thus arranged in some particular orientation, related to the frozen ground state. We would like to average over all possible orientations for these modes. In an infinite system this would be automatically done in the averaging over the quenched disorder, and one would expect a real glass to have spherically symmetric response functions.

An additional complication arises because there are (at least) two different angular averages:[15] one obtained from averaging the elastic constant c_{ijkl} and another from the compliance s_{ijkl}. Since it is easy in our case to do the latter analytically, we choose to average the compliance tensor. We have numerically checked that, for $x=0.5$, the two averages give values of λ/μ which differ by only

a fraction of 1%; the two results are significantly different,[16] however, for $x=0.7$.

We calculate the response to an external stress, averaging over an ensemble containing libration modes with all possible orientations. To perform the average in Eq. (13), we calculate $\langle C_{b,ij}C_{b,kl}\rangle$ where the angular brackets denote the above average. This is given by

$$\langle C_{b,ij}C_{b,kl}\rangle=\sum_{\mathbf{x},\alpha;\mathbf{y},\beta}M_{b,\mathbf{x}\alpha}M_{b,\mathbf{y}\beta}\frac{\partial^2}{\partial\xi_{\mathbf{x}\alpha}\partial\xi_{\mathbf{y}\beta}}\times\langle Q_{ij}(\mathbf{x})Q_{kl}(\mathbf{y})\rangle\ , \tag{14}$$

using (9). We now want to calculate $\langle Q_{ij}(\mathbf{x})Q_{kl}(\mathbf{y})\rangle$, which we will write in tensor form as

$$Q_{ijkl}\equiv Q_0^2[\hat{n}_i(\mathbf{x})\hat{n}_j(\mathbf{x})-\tfrac{1}{3}\delta_{ij}][\hat{n}_k(\mathbf{y})\hat{n}_l(\mathbf{y})-\tfrac{1}{3}\delta_{kl}]\ . \tag{15}$$

A simple way to calculate the spherical average of Q_{ijkl} is to use the fact that the most general isotropic fourth-rank tensor, which is symmetric under interchange of $i\leftrightarrow j$ and $k\leftrightarrow l$, and under $ij\leftrightarrow kl$, is given by

$$A_{ijkl}=B\delta_{ij}\delta_{kl}+C(\delta_{ik}\delta_{jl}+\delta_{il}\delta_{jk})\ . \tag{16}$$

Contracting A_{ijkl} with itself, we form the scalars $A_{ijij}=3B+12C$ and $A_{iijj}=9B+6C$. Performing these contractions with Q_{ijkl} gives

$$\begin{aligned}Q_{ijij}&=Q_0^2[(\hat{\mathbf{n}}_\mathbf{x}\cdot\hat{\mathbf{n}}_\mathbf{y})^2-\tfrac{1}{3}]\\ Q_{iijj}&=0\ ,\end{aligned} \tag{17}$$

and solving for Q_{ijkl} yields

$$Q_{ijkl}=\frac{Q_0^2}{30}[(\hat{\mathbf{n}}_\mathbf{x}\cdot\hat{\mathbf{n}}_\mathbf{y})^2-\tfrac{1}{3}](-2\delta_{ij}\delta_{kl}+\delta_{ik}\delta_{jl}+\delta_{il}\delta_{jk})\ . \tag{18}$$

Substituting the above result in (14), we find that the angular average $\langle C_{b,ij}C_{b,kl}\rangle$ is given by

$$\langle C_{b,ij}C_{b,kl}\rangle=\frac{Q_0^2A_b^2}{15}[-2\delta_{ij}\delta_{kl}+3(\delta_{ik}\delta_{jl}+\delta_{il}\delta_{jk})]\ , \tag{19}$$

where we have defined an average (dimensionless) coupling squared A_b^2 for each mode b by

$$A_b^2\equiv\tfrac{1}{2}\sum_{\mathbf{x},\alpha;\mathbf{y},\beta}M_{b,\mathbf{x}\alpha}M_{b,\mathbf{y}\beta}\frac{\partial^2}{\partial\xi_{\mathbf{x}\alpha}\partial\xi_{\mathbf{y}\beta}}(\hat{\mathbf{n}}_\mathbf{x}\cdot\hat{\mathbf{n}}_\mathbf{y})^2\ . \tag{20}$$

We note in passing that the longitudinal and transverse components of $\langle C_{b,ij}C_{b,kl}\rangle$ are given by

$$\langle C_b^2\rangle^{(\mathrm{L})}=\tfrac{4}{3}\langle C_b^2\rangle^{(\mathrm{T})}=\frac{4Q_0^2A_b^2}{15}\ . \tag{21}$$

For an isotropic medium, the compliance tensor is given by

$$s_{ijkl}=\frac{-\lambda}{2\mu(3\lambda+2\mu)}\delta_{ij}\delta_{kl}+\frac{1}{4\mu}(\delta_{ik}\delta_{jl}+\delta_{il}\delta_{jk})\ . \tag{22}$$

Performing the contraction in Eq. (13), and using (19) and (22), we find that the change in the compliance tensor due to mode b is given by

$$\Delta s_{ijkl}=\frac{A_b^2Q_0^2}{60VI\Omega_b^2\mu^2}[-2\delta_{ij}\delta_{kl}+3(\delta_{ik}\delta_{jl}+\delta_{il}\delta_{jk})]\ . \tag{23}$$

There is a sum rule for the coupling of external strains to the librations. Performing the derivatives, the sum over all the libration modes of A_b^2 is given by

$$\sum_{b=1}^{2N}A_b^2=\sum_{b=1}^{2N}\sum_{\mathbf{x},\alpha;\mathbf{y},\beta}M_{b,\mathbf{x}\alpha}M_{b,\mathbf{y}\beta}\left[\left[\frac{\partial\hat{\mathbf{n}}_\mathbf{x}}{\partial\xi_{\mathbf{x}\alpha}}\cdot\hat{\mathbf{n}}_\mathbf{y}\right]\left[\hat{\mathbf{n}}_\mathbf{x}\cdot\frac{\partial\hat{\mathbf{n}}_\mathbf{y}}{\partial\xi_{\mathbf{y}\beta}}\right]+(\hat{\mathbf{n}}_\mathbf{x}\cdot\hat{\mathbf{n}}_\mathbf{y})\left[\frac{\partial\hat{\mathbf{n}}_\mathbf{x}}{\partial\xi_{\mathbf{x}\alpha}}\cdot\frac{\partial\hat{\mathbf{n}}_\mathbf{y}}{\partial\xi_{\mathbf{y}\beta}}\right]\right]\ . \tag{24}$$

Since M is an orthogonal matrix with $\sum_b M_{b,\mathbf{x}\alpha}M_{b,\mathbf{y}\beta}=\delta_{\mathbf{x}\alpha,\mathbf{y}\beta}$, the sum over b is trivial. Then the first term in the large square brackets vanishes and (24) simplifies to

$$\sum_{b=1}^{2N}A_b^2=\sum_{\mathbf{x},\alpha}\left[\frac{\partial\hat{\mathbf{n}}_\mathbf{x}}{\partial\xi_{\mathbf{x}\alpha}}\right]^2=\sum_{\mathbf{x}}2=2N\ . \tag{25}$$

So A_b^2 averages to 1.

Just as we averaged the DOS of librations over various random configurations, we also average the coupling A_b^2. Averaging over all the modes in different realizations with frequency $\Omega_b=\Omega$ defines $A^2(\Omega)$, the mean-squared coupling of libration modes of frequency Ω to long-wavelength phonons. This quantity will be important later in calculating the scattering rate of phonons, as well as the zero-frequency shift in elastic constants. From Fig. 3 we see that there is a strong increase[17] in the coupling $A^2(\Omega)$ for the low-frequency librations.

B. Softening

We shall now discuss the physics of the elastic-constant renormalization due to the coupling of the harmonic libration excitations to the external strain fields.

It turns out that for all the properties concerning the harmonic excitations, the defect parameters Q_0, the dipole moment, and the moment of inertia, I, always appear in the same combination, Q_0^2/I. We will define this combination (pronounced lăm-mōm′) as

$$\Upsilon\equiv\frac{Q_0^2}{I}\ . \tag{26}$$

We write the sum over the libration modes in (13) in terms of the density of states per unit volume, $p(\Omega)$, using the replacement $V^{-1}\sum_b\rightarrow\int d\Omega\,p(\Omega)$. Then, using (22) and (23), the spherically symmetrized, renormalized compliance tensor can now be written as

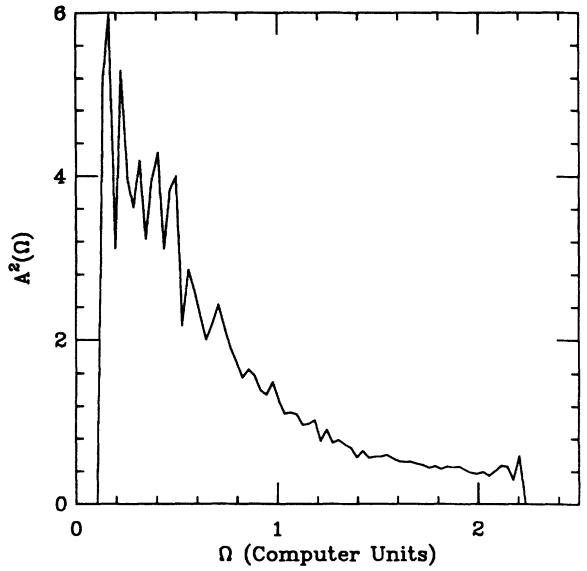

FIG. 3. The average coupling squares $\overline{A^2(\Omega)}$ of defect libration modes to long-wavelength phonons plotted as a function of libration frequency.

$$s_{ijkl}(0)=\left[\frac{-\lambda}{2\mu(3\lambda+2\mu)}-\frac{B}{30\mu}\right]\delta_{ij}\delta_{kl}+\left[\frac{1}{4\mu}+\frac{B}{20\mu}\right](\delta_{ik}\delta_{jl}+\delta_{il}\delta_{jk}) , \tag{27}$$

where we have defined the dimensionless parameter

$$B\equiv\frac{\Upsilon}{\mu}\int d\Omega\frac{p(\Omega)A_b^2}{\Omega^2} . \tag{28}$$

If we now want to calculate the change in the Lamé coefficients, we must invert the s_{ijkl} tensor. Doing this gives softened Lamé coefficients[18] of

$$\lambda(0)=\frac{\lambda+(B/5)(\frac{2}{3}\mu+\lambda)}{1+B/5} ,$$
$$\mu(0)=\frac{\mu}{1+B/5} . \tag{29}$$

In these equations, λ and μ are the bare values.

From (29) we can see that the presence of the defects leads to a softening of the medium. The defects relax in response to the externally applied static stress, and thus the strain produced for a given stress is larger. Even though λ increases from its high-frequency value, the material is really getting softer. This can be seen from the fact that both the longitudinal and transverse speeds of sound decrease at low frequencies, since they are given by $v_T=\sqrt{\mu/\rho}$ and $v_L=\sqrt{(\lambda+2\mu)/\rho}$.

Note that if we apply hydrostatic pressure, the dipoles do not relax, since their relative orientations to each other do not change. Therefore we expect that the bulk modulus, $K=\lambda+\frac{2}{3}\mu$, should be unchanged, despite the presence of elastic dipoles. As can be verified from Eq. (29), K is unchanged by the presence of the defects; that is,

$$\lambda(0)+\tfrac{2}{3}\mu(0)=\lambda+\tfrac{2}{3}\mu . \tag{30}$$

TABLE I. Elastic data from De Yoreo, Ref. 5. Note that the bulk modulus K is quite constant over the entire range of concentrations for which the material is cubic.

x	c_{11}	c_{12}	c_{44} (10^{11} dyn/cm^2)	K
0	4.17	0.52	0.520	1.74
0.05	3.40	0.75	0.380	1.63
0.10	3.20	0.85	0.350	1.63
0.25	3.01	1.00	0.306	1.67
0.50	2.84	1.10	0.240	1.68

We can check to some degree whether the bulk modulus is independent of the concentration of defects by looking at KBr:KCN. If the cyanides are responsible for the change in elastic constants in this material, we expect that K should not change much as x is varied. The bulk modulus of a cubic material is given by $K=\frac{1}{3}C_{11}+\frac{2}{3}C_{12}$. In $(KBr)_{1-x}(KCN)_x$, as x changes from 0 to 0.5 (for the next-higher concentration, 0.7, the material is no longer cubic), the cubic elastic constants all change significantly (see Table I). C_{11}, which changes by the smallest factor, varies by 47% from its value at $x=0$. The bulk modulus, however, only changes by 6.5% over the same range of x.

IV. FINITE-FREQUENCY RESPONSE

We will now look at the coupling of finite-frequency phonons ($\omega\neq 0$) to the libration modes of the system. This discussion generalizes the analysis of static distortions coupled to the defect normal modes. The new feature is that, in addition to a shift in the elastic constants, which is now frequency (ω) dependent, we also obtain a dissipative part to the response which represents a phonon lifetime due to resonant scattering from the librations. The latter effect will play a crucial role in our understanding of thermal transport.

We begin with the energy of coupling between the elastic distortion in the medium to the local stress fields of the defects (located at $\mathbf{x}$),

$$H_{\text{interaction}}=-\sum_{\mathbf{x}} Q_{ij}(\mathbf{x})\varepsilon_{ij}^{E}(\mathbf{k},\eta)e^{i\mathbf{k}\cdot\mathbf{x}} , \tag{31}$$

where $\mathbf{k}$ and η are the wave vector and polarization of the distortion, and the superscript E denotes the fact that the strain field ε_{ij}^{E} is that caused by the externally applied stress σ_{ij}^{E}, so that

$$\varepsilon_{ij}^{E}=s_{ijkl}\sigma_{kl}^{E} . \tag{32}$$

Now, as argued earlier, the only important degrees of freedom of the defect system, for our purposes, are the small angular oscillations of the defects about their frozen orientations. We now go through the same sequence of steps as in the preceding section to arrive at the phonon-defect mode coupling. We first linearize (31) in the defect coordinates and then use (5) to write it in terms

of the normal modes. Generalizing our earlier equation, (9), we define the coupling constant $C_{b,ij}(\mathbf{k})$ of a phonon with wave vector $\mathbf{k}$ to the bth defect mode by

$$C_{b,ij}(\mathbf{k}) \equiv \sum_{\mathbf{x},\alpha} M_{b,\mathbf{x}\alpha} \frac{\partial Q_{ij}(\mathbf{x})}{\partial \xi_{\mathbf{x}\alpha}} e^{i\mathbf{k}\cdot\mathbf{x}} . \tag{33}$$

Using this, we obtain

$$H_{\text{interaction}} = \sum_{b=1}^{2N} C_{b,ij}(\mathbf{k}) \psi_b \varepsilon_{ij}^E(\mathbf{k},\eta) . \tag{34}$$

Equation (34) represents the interaction energy of a system of harmonic oscillators—the libration modes ψ_b with frequencies Ω_b and moments of inertia I—which are driven by the externally produced strain field,

$$\varepsilon_{ij}^E(\mathbf{k},\eta) = \tfrac{1}{2}(k_i\eta_j + k_j\eta_i)\varepsilon_0 e^{i\omega t} . \tag{35}$$

Consider now a single libration mode b; its induced amplitude under the effect of the external strain field is

$$\psi_b = -\frac{C_{b,ij}}{I} \chi(\omega;\Omega_b) \varepsilon_{ij}^E , \tag{36}$$

where the complex susceptibility $\chi(\omega;\Omega_b)$ is given by the usual expression for a harmonic oscillator:

$$\chi(\omega;\Omega_b) \equiv [(\Omega_b^2 - \omega^2) + i\omega\Gamma(\omega)]^{-1} \tag{37}$$

$$\equiv \chi'(\omega;\Omega_b) - i\chi''(\omega;\Omega_b) . \tag{38}$$

Note that the harmonic nature of the librations leads to a temperature-independent response.[19] The width of the resonance, $\Gamma(\omega)$, is given by

$$\Gamma(\omega) = \left[\frac{2}{3v_L^5} + \frac{1}{v_T^5} \right] \frac{\Upsilon A_b^2 \omega^2}{10\pi\rho} , \tag{39}$$

and is the inverse lifetime of the libration mode due to its coupling to the phonon bath. We take the Ω_b appearing in (37) to be the renormalized libration frequency, which takes into account the effects of the high-frequency phonons via an effective moment of inertia. Thus we do not need to keep an explicit shift[20] in the bare-libration-mode frequency from the coupling to the phonons.

We now calculate the effect of the libration modes on the elastic medium as before. Substituting (36) into the interaction energy gives

$$-\frac{1}{I} \sum_b C_{b,ij}(\mathbf{k}) C_{b,kl}(-\mathbf{k}) \chi(\omega;\Omega_b) \varepsilon_{ij}^E (\varepsilon_{kl}^E)^* . \tag{40}$$

Comparing this to $\frac{1}{2}V\delta_{ijkl}\sigma_{ij}^E\sigma_{kl}^E$, we obtain the change in the compliance tensor of the medium due to the phonon-defect coupling,

$$\Delta s_{ijkl}(\omega) = \frac{-s_{iji'j'}s_{klk'l'}}{IV} \sum_b C_{b,i'j'}(\mathbf{k}) C_{b,k'l'}(-\mathbf{k}) \chi(\omega;\Omega_b) . \tag{41}$$

Since the susceptibility is complex, the change in the compliance tensor has a part which is in phase with the external perturbation and one that is out of phase. We shall show below that, in the usual way, the real (in-phase) part represents a change in the elastic constants of the medium and the imaginary (out-of-phase) part represents a lifetime for the phonon excitations.

Before proceeding to the final physical results, we need to simplify (41) into a more manageable form. We will first perform a spherical average over the libration modes in the system. The angular average $\langle C_{b,ij}(\mathbf{k}) C_{b,kl}(-\mathbf{k}) \rangle$ may be evaluated in much the same way as in the static case, provided we make the approximation that we can effectively take the limit $\mathbf{k} \to \mathbf{0}$. Since our libration modes have little resemblance to plane waves, we expect that their coupling to phonons will be qualitatively unchanged by including the spatial modulation of the phonon amplitude. In any case, our simulation is small compared to the phonon wavelengths of interest, so the $\mathbf{k}$ dependence of the coupling is not accessible to us. Our final results seem largely independent[17] of the detailed form of the couplings, so long as the overall magnitudes are roughly maintained.

With the above approximation the factor $\exp[i\mathbf{k}\cdot(\mathbf{x}-\mathbf{y})] \simeq 1$, and we obtain the same result as in the static case, namely

$$\langle C_{b,ij}(\mathbf{k}) C_{b,kl}(-\mathbf{k}) \rangle = \frac{Q_0^2 A_b^2}{15} [-2\delta_{ij}\delta_{kl} + 3(\delta_{ik}\delta_{jl} + \delta_{il}\delta_{jk})] , \tag{42}$$

The phonon wave vector does not appear on the right-hand side since we have taken the $\mathbf{k} \to \mathbf{0}$ limit.

Next, we denote the sum over the defect modes in (41) by an average over the libration DOS via the replacement $V^{-1}\sum_b \to \int d\Omega\, p(\Omega)$. Just as in the static case, we define a dimensionless quantity representing the change in elastic constants by

$$B(\omega) \equiv B'(\omega) - iB''(\omega) \equiv \frac{\Upsilon}{\mu} \int d\Omega\, p(\Omega) A^2(\Omega) \chi(\omega;\Omega) . \tag{43}$$

Written out explicitly, $B'(\omega)$ and $B''(\omega)$ are given by

$$B'(\omega) = \frac{\Upsilon}{\mu} \int d\Omega\, p(\Omega) A^2(\Omega) \frac{\Omega^2 - \omega^2}{(\Omega^2-\omega^2)^2 + \omega^2\Gamma^2(\omega)} \tag{44}$$

and

$$B''(\omega) = \frac{\Upsilon}{\mu} \int d\Omega\, p(\Omega) A^2(\Omega) \frac{\omega\Gamma(\omega)}{(\Omega^2-\omega^2)^2 + \omega^2\Gamma^2(\omega)} . \tag{45}$$

Finally, using Eq. (22), which gives the compliance tensor in terms of the Lamé coefficients, together with (42), we find that the change in the compliance tensor, Eq. (41), spherically averaged, reduces to

$$\Delta s_{ijkl} = \frac{B(\omega)}{60\mu} [-2\delta_{ij}\delta_{kl} + 3(\delta_{ik}\delta_{jl} + \delta_{il}\delta_{jk})] , \tag{46}$$

with $B(\omega)$ given by (43). Note that in the static limit ($\omega = 0$) we recover our earlier result.

A. Frequency-dependent elastic constants

We will now focus on the real and imaginary parts of (46). We will find it convenient to first work out the longitudinal (L) and transverse (T) components of the compliance tensor. For a general tensor with the symmetries of c_{ijkl} or s_{ijkl},

$$A_{ijkl}=B\delta_{ij}\delta_{kl}+C(\delta_{ik}\delta_{jl}+\delta_{il}\delta_{jk}) , \tag{47}$$

these are given by

$$A^{(\mathrm{L})}=B+2C \quad \text{and} \quad A^{(\mathrm{T})}=C , \tag{48}$$

where the L component is given by $i=j=k=l$, and the T component by $i=k\neq j=l$. Adding the real part of (46) to the bare compliance tensor, we obtain the frequency-dependent compliance tensor whose components are

$$s^{(\mathrm{L})}(\omega)=\frac{\lambda+\mu}{\mu(3\lambda+2\mu)}+\frac{B'(\omega)}{15\mu} \tag{49}$$

and

$$s^{(\mathrm{T})}(\omega)=\frac{1}{4\mu}+\frac{B'(\omega)}{20\mu} . \tag{50}$$

It is then straightforward to obtain the renormalized (frequency-dependent) Lamé coefficients which are given by

$$\mu(\omega)=\frac{\mu}{1+\frac{1}{5}B'(\omega)} \tag{51}$$

and

$$\lambda(\omega)=\frac{\lambda+\frac{1}{5}(\lambda+\frac{2}{3}\mu)B'(\omega)}{1+\frac{1}{5}B'(\omega)} . \tag{52}$$

It is easy to check that in the static limit we obtain the same result for the "soft" Lamé coefficients as in the previous analysis. Also, in the limit $\omega\rightarrow\infty$, i.e., for phonon frequencies much larger than the characteristic libration frequencies, $B'(\omega)\rightarrow 0$, and the renormalized Lamé coefficients are simply equal to the "bare" λ and μ.

From the Lamé coefficients we can determine the longitudinal and transverse speeds of sound, which are

$$v_{\mathrm{L}}=\left[\frac{\lambda+2\mu+\frac{1}{5}(\lambda+\frac{2}{3}u)B'(\omega)}{\rho[1+\frac{1}{5}B'(\omega)]}\right]^{1/2} , \tag{53}$$

$$v_{\mathrm{T}}=\left[\frac{\mu}{\rho[1+\frac{1}{5}B'(\omega)]}\right]^{1/2} . \tag{54}$$

We calculate a mean sound velocity as a function of frequency by $\bar{v}^{-3}=\frac{1}{3}(v_{\mathrm{L}}^{-3}+2v_{\mathrm{T}}^{-3})$,

$$\bar{v}(\omega)=\left[\frac{\mu(\omega)}{\rho}\right]^{1/2}\left\{\frac{1}{3}\left[2+\left[\frac{\mu(\omega)}{\lambda(\omega)+2\mu(\omega)}\right]^{3/2}\right]\right\}^{-1/3} \tag{55}$$

for an isotropic medium. Here we are treating the material as if it had no dispersion, so that in the absence of the libration modes the sound velocity would be independent of frequency.

B. Phonon scattering

We now turn to the imaginary part of the compliance tensor (46). This is directly related to the rate of energy absorption per unit volume of the medium,

$$\frac{dE}{dt}=\omega\,\mathrm{Im}(s_{ijkl})\sigma_{ij}^{E}\sigma_{kl}^{E} , \tag{56}$$

where the externally applied stress field σ_{ij}^{E} has an $e^{i\omega t}$ time dependence. Using our earlier results, this may be rewritten as

$$\frac{dE}{dt}=\frac{\omega B''(\omega)}{\mu}(-\tfrac{1}{30}\sigma_{ii}\sigma_{jj}+\tfrac{1}{10}\sigma_{ij}\sigma_{ij}) . \tag{57}$$

Again, we find it convenient to look separately at the longitudinal and transverse cases. We will consider the phonon to be a strain field as in Eq. (35). It should be noted that a longitudinal phonon traveling in the, say, $\hat{\mathbf{x}}$ direction will have only an xx component in its strain field, but will have all three diagonal elements of its stress field nonzero.

For a longitudinal mode, $\sigma_{ii}=\eta k(3\lambda+2\mu)$, and $\sigma_{ij}\sigma_{ji}=\eta^2k^2(3\lambda^2+4\lambda\mu+4\mu^2)$, where η is the amplitude. Using this, we find that

$$\frac{dE^{(\mathrm{L})}}{dt}=\tfrac{4}{15}\omega B''(\omega)\eta^2k^2\mu . \tag{58}$$

For a transverse mode, $\sigma_{ii}=0$, and $\sigma_{ij}\sigma_{ji}=2\eta^2k^2\mu^2$, giving

$$\frac{dE^{(\mathrm{T})}}{dt}=\tfrac{4}{5}\omega B''(\omega)\mu\eta^2k^2 . \tag{59}$$

The mean free path $l=v\tau$, where τ is the corresponding phonon lifetime, is given by

$$(v\tau)^{-1}=l^{-1}=\frac{dE}{dt}\Big/\Phi , \tag{60}$$

where Φ is the incident energy flux. The energy flux of an elastic wave is given by

$$\Phi=\sigma_{ij}\frac{\partial u_j}{\partial t} , \tag{61}$$

which for longitudinal or transverse waves in an isotropic medium becomes

$$\Phi^{(\alpha)}=c^{(\alpha)}(\varepsilon^{(\alpha)})^2v_{\alpha} , \tag{62}$$

where the label α can take on values L and T, and $c^{(\mathrm{L})}=\lambda+2\mu$ and $c^{(\mathrm{T})}=\mu$. We find that the scattering rates for L and T phonons are given by

$$\frac{1}{\tau^{(\mathrm{L})}(\omega)}=\frac{4}{15}\frac{\mu}{\lambda+2\mu}\omega B''(\omega) \tag{63}$$

and

$$\frac{1}{\tau^{(\mathrm{T})}(\omega)}=\tfrac{1}{5}\omega B''(\omega) . \tag{64}$$

Finally we define an "average" phonon-scattering rate from librations,

$$\frac{1}{\tau_{\rm lib}(\omega)}=\frac{1}{3}\left[\frac{1}{\tau^{(\rm L)}(\omega)}+\frac{2}{\tau^{(\rm T)}(\omega)}\right] . \tag{65}$$

From (45) we see that $B''(\omega)$, and hence the phonon-scattering rates, are highly peaked functions of the phonon frequency. This peaked nature follows from the result that the scattering rate is obtained by a convolution of two peaked functions: the line shape $\chi''(\omega;\Omega)$ for resonant scattering off a single libration mode, and the peaked density of states $p(\Omega)$ for these modes. Note also that the phonon-scattering rate is temperature independent; as mentioned earlier, this is a direct consequence of the harmonic nature of the librations from which the phonons are scattered. We will see that this strong scattering leads to the plateau in the thermal conductivity.

V. SPECIFIC HEAT—TOTAL DENSITY OF HARMONIC EXCITATIONS

The low-temperature specific heat of glasses has two features which are rather different from crystalline materials. The first is the large specific heat below 1 K which has an almost linear temperature dependence. This part of the specific heat has a slow logarithmic time dependence. Due to finite-size limitations, we are unable to study within our simulation the very rare (few tens in a million) two-level systems, if they exist, or some alternative[21] nonphonon long-wavelength collective modes. Thus we will simply use the standard TLS phenomenology for $T<1$ K.

The second characteristic feature of glasses is the excess specific heat in the 1–10-K region, seen as a bump in C/T^3. Experimentally, this contribution appears to be time independent[1] and thus qualitatively different from the linear term. We will show that the harmonic libration modes have a peaked density of states which explains this excess specific heat.

Naively, it might seem that just adding the libration DOS to the Debye density of states ($\sim\omega^2$) for the acoustic phonons would give the bump in C/T^3. This is qualitatively correct: one does indeed get a bump in a plot of C/T^3, but the value of C/T^3 at temperatures above the bump is much too high, e.g., in KBr:KCN. The reason why one cannot simply add the Debye phonon and libration DOS is that the presence of the defects produces a considerable softening of the medium, as discussed in Sec. III, and this must be taken into account. The main effect of this phonon-defect coupling on the phonon density of states is the following. For phonon frequencies well below the characteristic libration frequencies, one must use the phonon DOS coming from the measured (from our point of view, "soft") speeds of sound. However, for phonon frequencies much larger than the librations, the dipoles no longer relax to take up the stress, and the medium appears hard relative to the measured elastic constants. The high-frequency phonon DOS is therefore considerably less than would be expected from the measured speeds of sound. This, as might be expected, has a significant impact upon the C/T^3 fits.

We estimate the above modification of the phonon DOS in a simple way by using the frequency-dependent sound velocity of Eq. (55). We assume that we can approximate the phonon dispersion relation by three polarizations all having the same dispersion. We then obtain the phonon density of states $g_{\rm ph}(k)=12\pi k^2(1/8\pi^3)$ per unit volume, or, equivalently,

$$g_{\rm ph}(\omega)=\frac{3k^2(\omega)}{2\pi^2}\frac{dk}{d\omega} . \tag{66}$$

Using $k(\omega)=\omega/\bar{v}(\omega)$, with $\bar{v}$ given by (55), we get

$$g_{\rm ph}(\omega)=\frac{3\omega^2}{2\pi^2\bar{v}^3(\omega)}\left[1-\frac{\omega}{\bar{v}(\omega)}\frac{d\bar{v}(\omega)}{d\omega}\right] . \tag{67}$$

Note from the above discussion that $\bar{v}(\omega)$ has a low value as $\omega\to 0$ and a high value as $\omega\to\infty$. In both these limits the second term in the parentheses is small compared with unity, and one obtains a Debye-like DOS, except with different speeds of sound. In between these two limits, $\bar{v}(\omega)$ goes from one value to the other in a nonmonotonic manner (see Fig. 5), and the second term is no longer negligible. However the details of this "crossover" in the phonon DOS are not very important, since in the *total* density of harmonic excitations the defect modes dominate precisely in this frequency range.

To calculate the total DOS for harmonic excitations, $g_{\rm total}(\omega)$, phonons plus defect modes, we make the approximation of simply adding the modified phonon DOS, (67), to the libration DOS, $p(\Omega)$. The specific heat of the elastic dipole glass is then given by the sum of the contributions from the TLS and the harmonic excitations, i.e., phonons plus librations:

$$C(T)=A_{\rm TLS}T+k_B\int d\omega\, g_{\rm total}(\omega)\frac{x^2e^x}{(e^x-1)^2} ,$$

$$g_{\rm total}(\omega)=g_{\rm ph}(\omega)+p(\omega) \tag{68}$$

where $x=\hbar\omega/k_BT$. The linear contribution from the TLS which dominates below 1 K has a coefficient $A_{\rm TLS}$ which is obtained from fitting the low-temperature data. We will compare the specific heat thus obtained with experiments in Sec. VII.

VI. THERMAL TRANSPORT

Our aim here is to calculate thermal transport for the elastic dipole model. We show that the resonant scattering of acoustic phonons from the libration modes, studied in Sec. IV above, leads to a plateau in the thermal conductivity.

Starting from the phonon Boltzmann equation, the thermal conductivity is given by the well-known result

$$\Lambda(T)=\int_0^{\omega_D}d\omega\, C_{\rm ph}(\omega,T)v^2\tau(\omega,T) . \tag{69}$$

In this expression,

$$C_{\rm ph}(\omega,T)=\frac{\omega^2}{2\pi^2v^3}\frac{k_Bx^2e^x}{(e^x-1)^2},\quad x=\hbar\omega/k_BT \tag{70}$$

is the specific heat of the phonons of frequency ω at temperature T, τ is their lifetime, or inverse scattering rate,

and v is the Debye speed of sound. We approximate the (total) scattering rate of a phonon by using Matthiesen's rule of adding the rates due to independent mechanisms.

There are three well-known mechanisms of phonon scattering in glasses and, as is well known,[7,22,23] these are inadequate to explain the thermal-conductivity plateau. They are resonant scattering from TLS, relaxational scattering from TLS, and Rayleigh scattering from density or elastic-constant fluctuations. For completeness, we briefly describe these mechanisms, since different scattering mechanisms determine the thermal conductivity in different temperature regimes. This will help in understanding the role[7] of the libration modes in producing the plateau.

A. Scattering from two-level systems

At very low temperatures the dominant scattering mechanism is resonant scattering from the TLS. This gives a scattering rate of[2]

$$\tau_{\rm res}^{-1}(\omega,T)=\frac{\pi\bar{\gamma}^{2}\bar{P}}{\rho v^{2}}\omega\tanh(\hbar\omega/2k_{B}T)$$
$$\equiv A\,\omega\tanh(\hbar\omega/2k_{B}T)\ , \qquad (71)$$

where $\bar{\gamma}$ is the strain coupling of TLS to phonons, $\bar{P}$ the density of TLS, and ρ the density of the material. Resonant scattering from the two-level systems gives a thermal conductivity proportional to T^2 at low temperatures, in agreement with experiments below 1 K.

Another scattering mechanism involving the TLS is relaxational scattering.[24,25] This is due to the fact that a phonon modulates the energy splitting of the TLS, and the TLS populations try to stay in equilibrium via the emission and absorption of phonons. An approximate expression for the resulting phonon lifetime is[23]

$$\tau_{\rm rel}(\omega,T)=\frac{1}{aT^{3}}+\frac{1}{b\omega}\ . \qquad (72)$$

The parameters a and b are given by

$$a=\frac{\pi^{3}\bar{P}\bar{\gamma}^{4}k_{B}^{3}}{8\rho^{2}\hbar^{4}v^{7}},\quad b=\frac{\pi\bar{P}\bar{\gamma}^{2}\omega}{2\rho v^{2}}=A/2\ .$$

The first term in (72) dominates at low temperature, when the TLS are relaxing slowly on the scale of the incident-phonon frequency ω, and the second term (which will be more important for us below) takes over a high temperatures when the TLS relax fast compared with ω. Relaxational scattering plays no role in low-temperature thermal transport (see, e.g., Ref. 23), and is only observable in ultrasound experiments[25] where the resonant interaction is saturated by a large acoustic intensity.

B. Rayleigh scattering

At high temperatures ($T>10$ K), Rayleigh scattering, with its strong frequency dependence, is the dominant mechanism. The Rayleigh-scattering rate cannot grow indefinitely as ω^4 and we will cut it off by simply assuming that the mean free path must be larger than interatomic distances. The scattering rate is given by

$$\tau_{\rm Rayl}^{-1}(\omega)=\left[\tau_{\rm min}+\frac{1}{R\omega^{4}}\right]^{-1}\ , \qquad (73)$$

where

$$R=\frac{a_{0}^{3}F\omega^{4}}{4\pi v^{3}}\ . \qquad (74)$$

Here, a_0 is the microscopic length scale on which the density or elastic-constant fluctuations occur, and F characterizes the magnitude of these fluctuations. $\tau_{\rm min}\sim a_0/v$ ensures that the mean free path does not become smaller than a_0.

The thermal conductivity calculated from adding the phonon scattering from the above three mechanisms, i.e., using $\tau^{-1}(\omega,T)=\tau_{\rm res}^{-1}(\omega,T)+\tau_{\rm rel}^{-1}(\omega,T)+\tau_{\rm Rayl}^{-1}(\omega)$ in (69), is about an order of magnitude too large in the 1–10-K region, and does not explain the plateau. (See, e.g., Fig. 3 of Ref. 6, or Fig. 4 of Ref. 7.) In other words, these three mechanisms together produce too little phonon scattering to cause the plateau.

Estimates of the Rayleigh coefficient R have varied in the literature. Microscopic estimates[26] for, e.g., vitreous silica give too little Rayleigh scattering to give the plateau. In the glassy crystal KBr:KCN these estimates[7] are even more straightforward, and are again found to be too small. However, it has been pointed out by a number of authors that if R is treated as a free parameter, and chosen to be 2 orders of magnitude larger than the earlier estimates, then this alone can give a plateau. In Ref. 27 it was argued that this increased value of R is due to the existence of a new correlation length in glasses. However, there is little independent evidence for such a length scale, say from structural studies. (We will discuss other proposals for the thermal conductivity plateau in Sec. X, after describing our own calculations.)

C. Scattering from librations: Thermal-conductivity plateau

In addition to the above mechanisms, we next include the phonon scattering from the librations which we have described in Sec. IV. This introduces the following changes in the thermal-conductivity calculation using (69). First, we take the total scattering rate in (69) to be the sum of the rates due to TLS scattering, libration scattering, and Rayleigh scattering:

$$\tau^{-1}(\omega,T)=\tau_{\rm res}^{-1}(\omega,T)+\tau_{\rm rel}^{-1}(\omega,T)+\tau_{\rm Rayl}^{-1}(\omega)+\tau_{\rm lib}^{-1}(\omega)\ . \qquad (75)$$

Second, we approximate the different phonon dispersion relations by that given from the frequency-dependent average speed of sound (55), so that $v=\bar{v}(\omega)$. Third, we use the same approximation for the phonon density of states that we had used for specific heat. We thus use

$$C_{\rm ph}(\omega,T)=\tfrac{1}{3}g_{\rm ph}(\omega)\frac{k_{B}x^{2}e^{x}}{(e^{x}-1)^{2}},\quad x=\hbar\omega/k_{B}T \qquad (76)$$

instead of (70). We should note that the first change, i.e., inclusion of the libration-scattering rate, is crucial; the second and third points do not make any qualitative

change in the results. In the next section we will show that with the libration scattering we obtain a plateau in thermal conductivity in good agreement with experiments.

Fits to the data will be discussed in the next section; here we shall describe the formation of the plateau. The basic idea is simply that the libration modes are excitations whose frequencies match the thermal phonons in the plateau regime. Resonant scattering of acoustic phonons from these libration modes then leads to the thermal-conductivity plateau. The detailed discussion below of the different scattering mechanisms dominating in different temperature regimes follows Ref. 7.

Below 1 K the phonons dominating thermal transport have frequencies much lower than those characteristic of the librations. The librations play no role there and the usual T^2 dependence of the thermal conductivity is obtained from resonant scattering from TLS with a broad distribution of energy splittings.

As we approach the plateau regime the libration DOS increases, and the modes begin to limit thermal transport. Between roughly 1 and 10 K the thermal phonons are extremely strongly scattered by the libration modes, and are practically not carrying any heat current at all. The current is then mainly being carried by the low-frequency phonons ($\hbar\omega \ll k_B T$) in the plateau region. This, incidentally, shows that the dominant phonon approximation, of equating temperature and frequency to obtain a scattering rate (or mean free path) from (69), is totally misleading. There is no way, in general, to deduce the frequency-dependent scattering rate from the measured temperature dependence of the thermal conductivity, since a broad distribution of phonons is responsible for transport.

The low-frequency phonons responsible for thermal transport in the plateau regime are limited by the (a) relaxational scattering, and (b) scattering from the low-frequency tail of the libration DOS. We have shown[7] that in the absence of these mechanisms, resonant scattering of the low-energy phonons from the TLS is not sufficient to create a plateau, and, in fact, leads only to a T^2-to-T crossover in the thermal conductivity. When (a) and (b) are included, however, one obtains a T^2-to-flat crossover, which is the onset of the plateau.

The upper edge of the plateau corresponds to a decrease in the libration DOS beyond its peak. This leads to an increase in the conductivity above the plateau. Above the plateau the thermal phonons are limited by Rayleigh scattering, which with its ω^4 dependence must dominate at sufficiently high frequencies. Eventually, this rise in the scattering rate is cut off once the phonon mean free path becomes as small as the interatomic spacing.

Rayleigh scattering is not necessary for the existence and the onset of the plateau in our model. In fact, if we turn off (by hand) Rayleigh scattering completely, we still get a start of a plateau. About halfway through the plateau, however, the thermal phonons start to have a higher frequency than the libration modes. Then, since these phonons are not strongly scattered by anything, the thermal conductivity abruptly increases very sharply.

VII. COMPARISON WITH EXPERIMENTS

We now turn to comparing the results obtained from our model with experiments, first for the orientational glass KBr:KCN and then for vitreous silica. Some of the details of transforming the parameters used in the computer simulation of the elastic dipole model to real physical units are discussed in the Appendix.

A. KBr:KCN

KBr:KCN was the motivation for our model of glasses, and is a material with which we can make rather direct comparison with experiment; as we will show, there are essentially no free parameters for KBr:KCN.

To turn the results of the simulation into real numbers, we need to know three things: (1) the density of defects $\equiv$ cyanide, for this material, (2) $\Upsilon = Q_0^2/I$ [see Eq. (26)], which characterizes a single dipole defect, and (3) the elastic constants. The first is trivially known[28] for $(\mathrm{KBr})_{1-x}(\mathrm{KCN})_x$ from the cyanide concentration x. This then determines the normalization of the libration density of states.

The second, Υ is also experimentally known since both the elastic dipole moment and the moment of inertia of a CN^- ion in a KBr host have been measured. It turns out that neither value is known very precisely (see below), so that the resulting value for Υ is probably only known within a factor of 2 or so. However, the characteristic libration frequency, and hence the location of the bump in specific heat and the thermal-conductivity plateau, scale only as $\sqrt{\Upsilon}$, so that various choices of this parameter do not lead to qualitatively different results. (Compare this with other theories of the plateau which have to tune parameters, e.g., the Rayleigh-scattering amplitude, by an order of magnitude or more to get a plateau at all.)

The elastic dipole moment is obtained as follows. The "shape factor" λ_s (see Ref. 29) measured in the stress-dichroism experiment of Beyeler[30] is related to the elastic dipole tensor via $Q_{\alpha\beta} = c_{\alpha\beta\mu\nu}\Lambda_{\mu\nu}$, where $\Lambda_{\mu\nu} = \lambda_s V_0(\hat{n}_\mu \hat{n}_\nu - \frac{1}{3}\delta_{\mu\nu})$, where V_0 is the primitive cell volume. Thus we find that the elastic dipole moment Q_0 is given by $Q_0 = 2\lambda_s V_0 \mu$, where all of the quantities on the right-hand side are experimentally measured.

We estimate $Q_0 \simeq 1.3$ eV, using the measured[30] shape factor $\lambda_s \simeq 0.2$, the volume of the primitive cell $V_0 = 72$ Å^3, and approximating $\mu \simeq 7.3\times 10^{10}$ dyn/cm^2 for KBr. This value of μ is obtained by the Reuss average,[15] which is the spherical average of the compliance tensor of KBr (which has cubic symmetry). The Voigt average,[15] which is an average of the elastic moduli, yields an estimate of $\mu \simeq 10.4\times 10^{10}$ dyn/cm^2, with a correspondingly higher estimate of Q_0.

The moment of inertia of a cyanide in a KBr host estimated from the rotational constant measured in one experiment[30] is $I = 2.8\times 10^{-39}$ g cm^2, though another[31] yields $I = 6.5\times 10^{-39}$ g cm^2.

As emphasized earlier, only the combination $\Upsilon = Q_0^2/I$ is needed to compute the low-temperature properties of interest. We have used a value of $\Upsilon = 1.1\times 10^{15}$ ergs/sec^2. For $Q_0 = 1.3$ eV this implies $I = 4.0\times 10^{-39}$

g cm^2, consistent with experiment.

The final physical quantity needed is the ratio of the "bare" elastic constants to the values used in the simulation. The experimentally measured constants are the low-frequency values, which, as we have seen, are softened by the presence of the dipoles. In the Appendix we show how to determine the bare elastic constants from the measured low-frequency speed of sound, Υ, and the density of defects. For $(KBr)_{1-x}(KCN)_x$ we will use this procedure to determine the bare elastic constants for $x=0.5$, and then use the same values of the bare elastic constants for all x values.

In Fig. 4 we show (1) the Debye-phonon density of states corresponding to the measured (low-frequency) speed of sound, (2) the phonon density of states $g_{ph}(\omega)$ of Eq. (67), which has been modified from the bare-phonon DOS due to the coupling to librations, and (3) the *total* density of harmonic excitations $g_{total}(\omega)$, which is the sum of curve (2) and the libration DOS [see Eq. (68)]. Note that the libration modes, seen as the bump in the total-DOS curve, are indeed lower in frequency than the majority of the phonon modes. This provides some justification of our approximation that the phonons relax much faster than the dipoles. However, a simple estimate of the time taken for a phonon to propagate between two neighboring defects shows that this time scale is only a factor of 2 or 3 shorter than the time period of a typical libration oscillation. Thus, at least for KBr:KCN, the neglect of retardation effects in the defect Hamiltonian must be treated only as a first approximation.

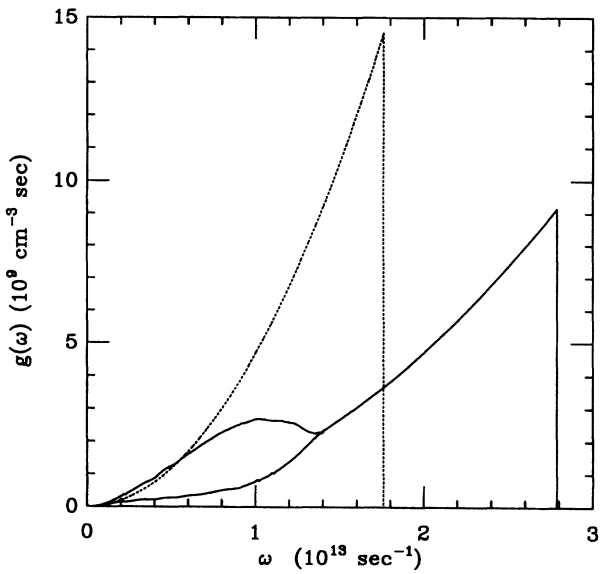

FIG. 4. The dashed curve is the Debye-phonon density of states (DOS) as determined from the measured low-frequency speed of sound for $x=0.5$. Also plotted is the phonon DOS, g_{ph}, modified due to interactions with the defects; see Eq. (67). At low frequencies this agrees with the dashed curve, but at high frequencies the effective speed of sound is higher, leading to a lower DOS. The third curve is the *total* density of harmonic excitations [see Eq. (68)], which is the modified phonon DOS plus the libration DOS, the latter showing up as the bump at intermediate frequencies. Note that the libration modes are significantly lower in frequency than the majority of the phonon modes. Thus our approximation of assuming that the phonons relax much faster than the dipoles is reasonable.

Figure 5 shows the frequency-dependent speed of sound predicted for $(KBr)_{0.5}(KCN)_{0.5}$. The two curves shown come from (a) setting the *high*-frequency speed of sound to be that given by using the elastic constants of KBr, and (b) setting the *low*-frequency speed of sound to be that given by using the speed of sound of $(KBr)_{0.5}(KCN)_{0.5}$. We thus find that the softening predicted from the elastic dipole model is in fairly good agreement with the experimental softening from the KBr values. Also recall the agreement between the data of Table I and the model: the relaxation of the dipoles leads to a softening of the shear modulus without affecting the bulk modulus.

We next plot the phonon-scattering rate in Fig. 6. As discussed earlier, the strongly peaked nature of this rate is due to resonant scattering from libration modes with a peaked DOS. At its peak the transverse scattering rate just exceeds the line $\omega\tau=1$, the Ioffe-Regel criterion for localization.[32] We have earlier argued in Ref. 7 that the plateau is *not* evidence for phonon localization. As shown there, inclusion of coherent multiple-scattering effects does not affect the thermal-transport results: a broadband measurement like thermal conductivity is insensitive to whether a narrow band of phonons is very strongly scattered or, in fact, localized, since all the heat is carried by other phonon modes anyway. If it becomes feasible at some future date to experimentally study monochromatic phonon propagation in the terahertz frequency region, the possibility of the two mobility edges may be tested.

In Table II we list the parameters used in calculating

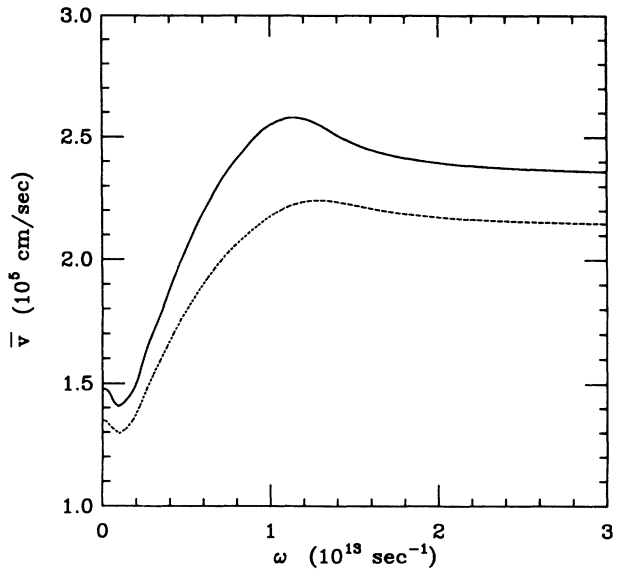

FIG. 5. Mean speed of sound as a function of frequency. The two curves are both for $x=0.5$. The bottom dashed curve has set the high-frequency speed of sound from the elastic constants of KBr. The top curve sets the low-frequency speed of sound to the correct value for $x=0.5$, 1.48×10^5 cm/sec. The two curves agree to about 15%.

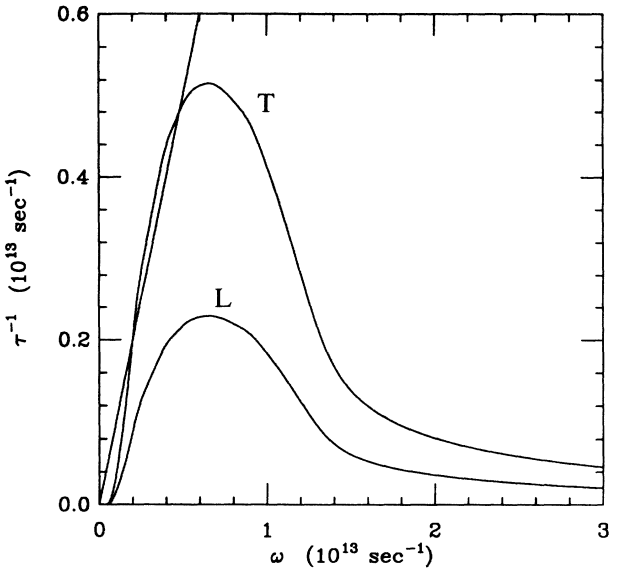

FIG. 6. Scattering rate of longitudinal and transverse phonons as a function of frequency. Also shown is the line $\tau^{-1}=\omega$, the Ioffe-Regel criterion for localization.

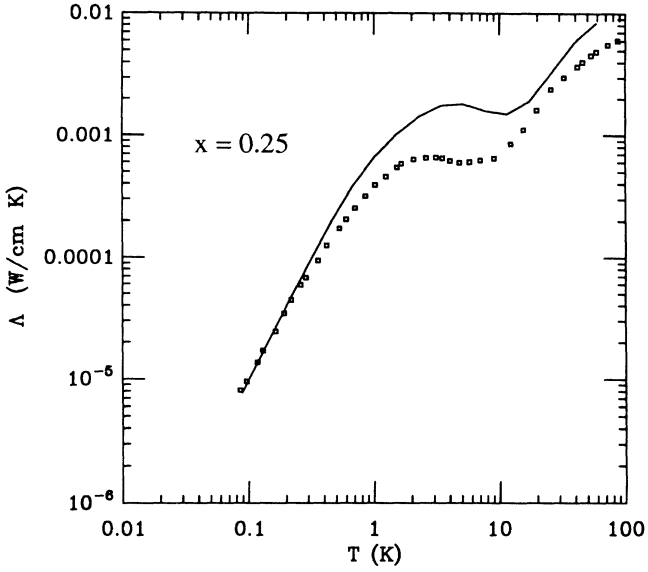

FIG. 7. Thermal conductivity for $x=0.25$. Solid line is calculated, as described in the text. The $(KBr)_{1-x}(KCN)_x$ experimental thermal-conductivity data for Figs. 7–9 are from Ref. 5.

the thermal conductivity and the specific heat. The TLS parameters are chosen, as usual, by fitting to the thermal data below 1 K; there are no other free parameters for KBr:KCN, as shown above.

Figures 7–9 show the thermal conductivity for the three concentrations $x=0.25,0.5,0.7$; the theoretical curves have been calculated using (69) together with (75) and (76). The plateaus in the thermal conductivity are in fairly good agreement with the experimental data. Since, as discussed earlier, the height of the plateau depends somewhat on where exactly the librations start limiting the current, it is sensitive to the shape of the libration DOS on the low-frequency side. This may explain the fact that our theoretical curves in the plateau region often have a thermal conductivity somewhat higher than the experimental value.

The specific heat of KBr:KCN and the model, obtained from (68), are shown in Figs. 10–12. The specific heat, especially when plotted as C/T^3, is much more sensitive to details of the distribution than the thermal conductivity. This is because, while the plateau in the thermal conductivity is caused by the majority of modes in the center of the distribution, the specific-heat bump is caused by the low-frequency tail of the distribution. The bump in C/T^3 results from the total density of states first starting to grow faster than ω^2, but soon beginning to grow slower than ω^2.

The C/T^3 curve for $x=0.7$, though qualitatively correct, is in rather poor agreement with that data, even though, surprisingly, the thermal-conductivity fit is excellent. Since we determined the bare elastic constants from $x=0.5$, the predicted soft speed of sound from the simulation for $x=0.7$ does not have to fit the experimental value, and, in fact, it does not. In the $x=0.7$ simulation there are some low-frequency modes that couple extremely strongly to the phonons, and these lead to a large softening; the predicted low-frequency (1.3×10^5 cm/sec) is quite a bit less than the experimental value (1.6×10^5 cm/sec). This difference may have to do with the fact that we have the wrong ground state (see I) at high con-

TABLE II. Parameters used in the calculation of the thermal conductivity and specific heat. The tunneling-system parameters for silica are derived from data given in De Yoreo *et al.* (Ref. 5). The data for SiO_2 are compiled from several sources (Refs. 9, 27, and 25).

	x			
Parameters	0.25	0.5	0.7	0.5 (SiO_2)
ρ (g/cm^3)	2.50	2.18	1.95	2.2
v_D (cm/sec)	1.54×10^5	1.48×10^5	1.63×10^5	4.1×10^5
g_{pho} (cm^{-3})	8.55×10^{22}	8.4×10^{22}	8.67×10^{22}	1.9×10^{23}
g_{lib} (cm^{-3})	7.13×10^{21}	1.4×10^{22}	2.02×10^{22}	1.0×10^{22}
Υ (ergs/sec^2)	1.11×10^{15}	1.11×10^{15}	1.11×10^{15}	4.0×10^{16}
TLS A	7.80×10^{-4}	4.79×10^{-4}	9.67×10^{-4}	8.92×10^{-4}
TLS relaxation a (sec^{-1}K^{-1})	2.96×10^5	7.01×10^5	5.96×10^6	4.0×10^5
Rayleigh R (sec^3)	7.50×10^{-41}	1.49×10^{-40}	1.20×10^{-40}	4.53×10^{-41}
Rayleigh τ_{min} (sec)	2.7×10^{-13}	2.7×10^{-13}	2.7×10^{-13}	4×10^{-14}
TLS specific heat (ergs/K^2)	24.0	9.0	4.3	10.0

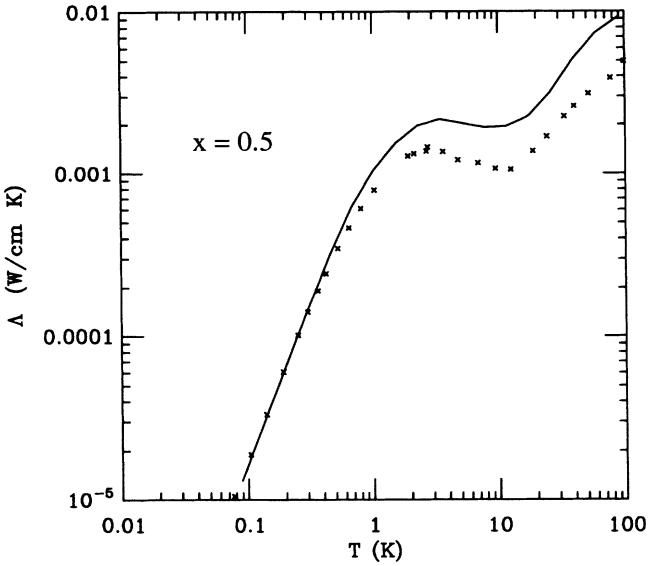

FIG. 8. Thermal conductivity for $x=0.5$ (see Fig. 7).

centrations.

It is also true that in glasses the bump in the specific heat varies much more from glass to glass than the plateau in the thermal conductivity. Also, most glasses have a bump in C/T^3 whose magnitude is much larger than the one in KBr:KCN. This may be seen by noting that KBr:KCN has a softer shear modulus than real glasses, and hence a considerably larger phonon density of states. Thus the relative contribution of the defect libration modes to the specific heat is correspondingly smaller.

B Vitreous silica

We now compare the results of the elastic dipole model with low-temperature data on vitreous silica. As we have emphasized earlier, ours is not a microscopic model for real glasses (see the discussion in Sec. II of I). However,

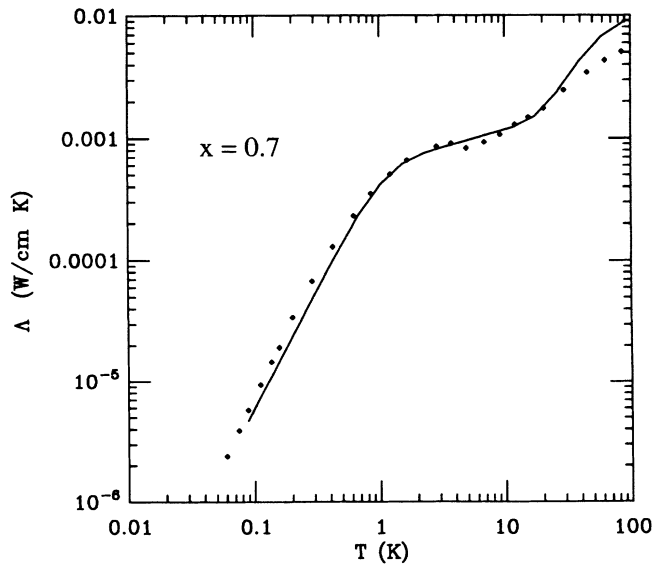

FIG. 9. Thermal conductivity for $x=0.7$ (see Fig. 7).

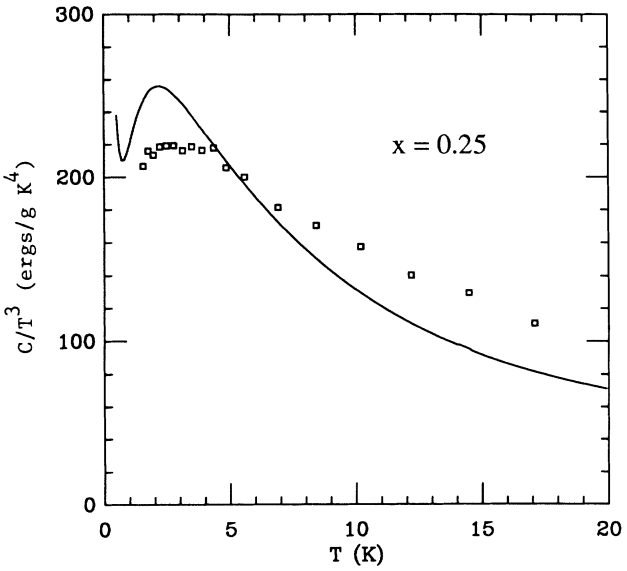

FIG. 10. C/T^3 for $x=0.25$. Solid line is calculated, as described in the text. The experimental $(KBr)_{1-x}(KCN)_x$ specific-heat data for Figs. 10–12 are from Ref. 47.

it is interesting to see to what extent it can serve as a phenomenological for structural glasses.

Recent inelastic-neutron-scattering experiments by Buchenau *et al.*[10] on vitreous silica show that there is a fairly large density of excess states (i.e., states in addition to the acoustic phonons) at frequencies of about 10^{13} rad/sec, which appear to be harmonic in nature and have localized eigenvectors. Buchenau *et al.*[10] have suggested that rotational motion of five coupled SiO_4 tetrahedra may be the origin of these low-frequency harmonic modes. The connection between the excess specific heat and these extra modes is immediately obtained as shown in Ref. 10. However, the connection with the thermal-conductivity plateau requires a model for phonon scatter-

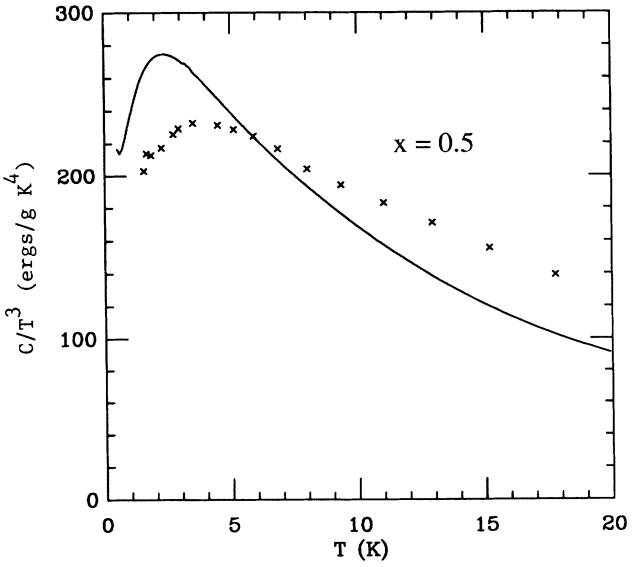

FIG. 11. C/T^3 for $x=0.5$ (see Fig. 10).

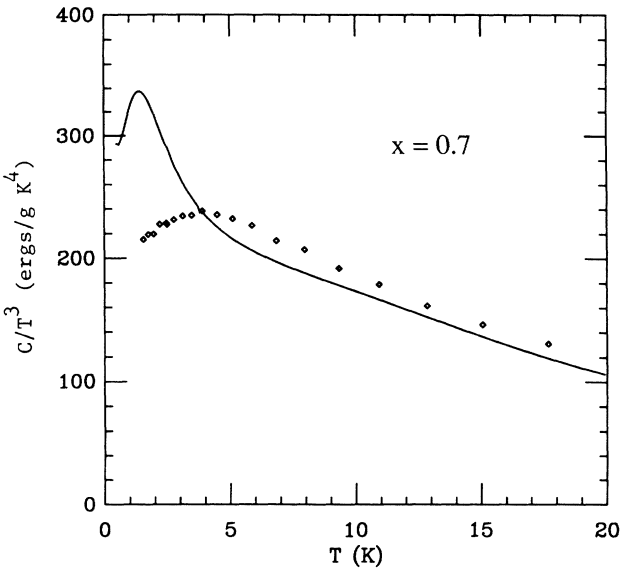

FIG. 12. C/T^3 for $x=0.7$ (see Fig. 10).

ing off these extra modes.

We use the elastic dipole model to make this connection. We determine the parameters of the model by comparing the total density of harmonic excitations in the model with the experimentally measured DOS. The height of the excess peak fixes the density of "defects" and the location of this peak determines the defect parameter Υ. In our model the same parameter Υ determines both the characteristic libration frequency and also the phonon scattering relevant for thermal transport. Thus once this parameter is fixed by the neutron DOS, the thermal conductivity can be calculated without any additional parameters. We cannot, of course, make any microscopic identification of what the "defects" are in a-SiO_2.

In Fig. 13 we match the total DOS from the elastic dipole model with the experimental curve; the corresponding values of the parameters are listed in Table II. From these values of the parameters, we obtain reasonable curves for the thermal conductivity and specific heat as shown in Figs. 14 and 15. The TLS parameters (see Table II) used were chosen, as usual, to fit the very-low-temperature data ($T<1$ K). The Rayleigh-scattering estimate of Ref. 26 (which by itself is unable to explain the plateau) was used.

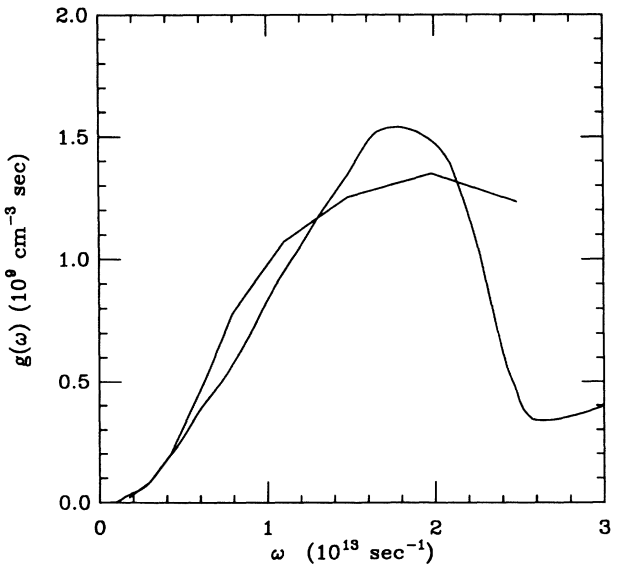

FIG. 13. Density of defect-libration-mode states from simulation fit to the neutron-scattering data of Ref. 10.

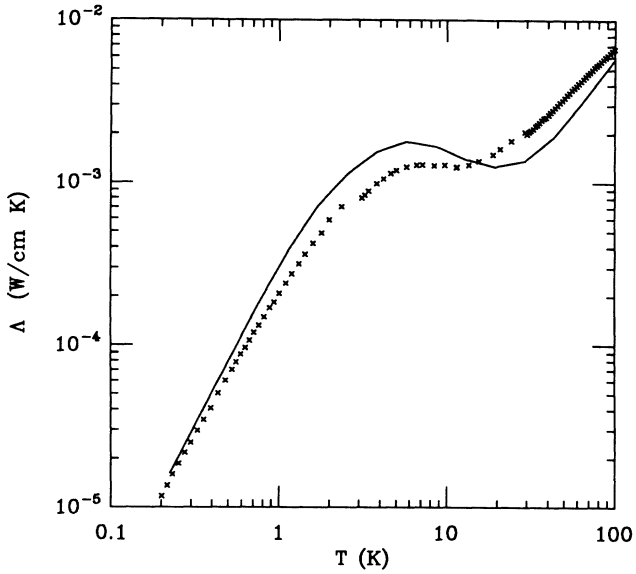

FIG. 14. Thermal conductivity calculated from the parameters used for SiO_2. Experimental values are from the Cornell group.

There are several comments that should be made about the use of the elastic dipole model to study thermal conductivity of vitreous silica. First, it shows that there was nothing special about the exact parameters used for

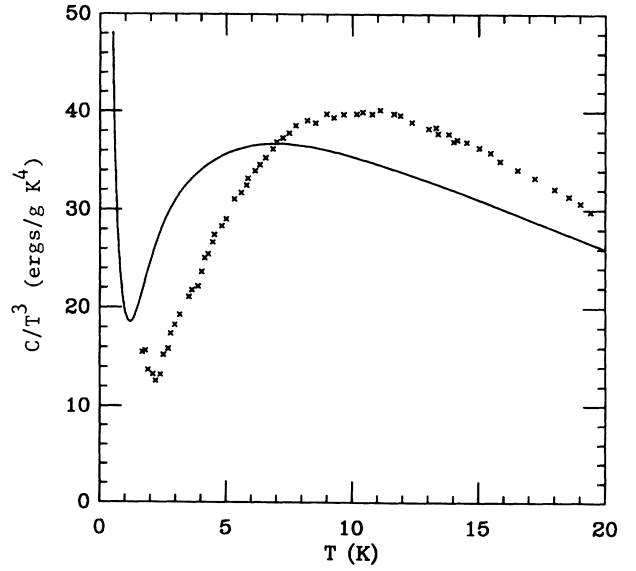

FIG. 15. Calculated specific heat plotted as C/T^3, and the experimental specific heat for SiO_2 from Ref. 10.

KBr:KCN, and that this model generically produces the universal intermediate-temperature glassy properties. To what extent the parameter values needed for a-SiO_2 are reasonable will be discussed in the following section.

Second, there has been a long-standing controversy about the role of Rayleigh scattering in producing the plateau in glasses. Our calculation shows that Rayleigh scattering has no effect on the existence and the onset of the plateau, as explained above.

Third, there was some evidence from early experiments[33] of monochromatic phonon propagation in a-SiO_2 that phonons in the 100–300-GHz frequency range undergo *inelastic* scattering. This would be in contradiction with our model since the resonant scattering from libration modes is *elastic,* in the sense that the scattered phonon has the same frequency as the incident one. However, more recent experiments[34] on samples free of impurities suggest that the scattering may, in fact, be elastic, so that there is no disagreement.

In conclusion, these results strongly suggest that the intermediate-temperature universal properties in various glasses are related to the existence of additional harmonic excitations in the tetrahertz frequency range.

VIII. UNIVERSALITY OF THE PLATEAU

We discussed the physics underlying the thermal-conductivity plateau at the end of Sec. VI. We now turn to two other issues related to the plateau in the elastic dipole model.

First, we discuss the universality of the plateau within this model, and the related universality of the softening of the shear modulus due to the presence of the defects. We show that strong scattering with $\omega\tau \sim 1$, and consequently a plateau, is always obtained within the interacting elastic dipole model, independent of the parameters of the model; the location of the plateau is, however, dependent on the parameters.

Second, we examine to the extent to which our model is successful in describing the universal low-temperature properties of real glasses. The above-mentioned universality is closely related to the assumption that the dynamics of the defects is determined only by their mutual interaction $1/r^3$ interactions. We discuss the validity of these assumptions in the context of our fits to the thermal data for a-SiO_2.

A. Universality of scattering and softening

A simple argument shows the existence of very strong phonon scattering in the elastic dipole model, independent of the concentration of defects and of the defect parameter Υ. To estimate the peak in the phonon scattering due to the librations, and show that it always has $\omega\tau$ of order unity, let us make some simplifying assumptions. Assume that the width of the resonance is much less than that of the librational density of states, and that $\overline{A^2}$ can be approximated by its average value of 1. In this case, Eq. (45), for the imaginary part of the compliance tensor $B''(\omega)$, can be integrated, giving

$$B''(\omega) \sim \frac{\pi \Upsilon p(\omega)}{2\mu\omega} . \tag{77}$$

The scattering rates for phonons, Eqs. (63) and (64), are equal to numerical factors of order unity times $\omega B''(\omega)$, so that

$$\tau(\omega) \sim \frac{\mu}{\Upsilon p(\omega)} . \tag{78}$$

Further, since the only energy scale in the model is the elastic interaction between dipoles, both the peak frequency and the width of the libration DOS, $p(\Omega)$, are proportional to

$$\overline{\Omega} \sim (\Upsilon/\mu a^3)^{1/2} , \tag{79}$$

where a is a typical distance between dipoles. Here, $\overline{\Omega}$ is a typical libration-mode frequency, or the frequency at which the density of libration modes peak. The total density of modes per unit volume is then proportional to

$$p(\overline{\Omega})\overline{\Omega} \sim 1/a^3 . \tag{80}$$

We now want to know how strong the scattering will be for phonons whose frequency $\bar{\omega}$ is approximately equal to $\overline{\Omega}$. Combining (78)–(80), we see that

$$\bar{\omega}\tau(\bar{\omega}) \sim 1 \quad \text{for } \bar{\omega} \simeq \overline{\Omega} , \tag{81}$$

independent of all the parameters. Thus we expect to always have very strong scattering close to the peak of the defect density of states.

As shown above, and discussed in Ref. 7, this strong scattering in a band of frequencies about $\overline{\Omega}$ leads[35] to a plateau in the thermal conductivity centered at a temperature which scales as $\overline{\Omega}$. Thus, while the existence of the plateau is a universal feature of the elastic dipole model, its location is not, since this depends upon the model parameters, as seen from (79).

A related universal feature of the elastic dipole model is in the real part of the change in the compliance of the medium, i.e., in the softening of the shear modulus. Let us discuss this in a slightly different way from the imaginary part above, though the basic idea is the same. As shown in the Appendix, the conversion between the computer frequency units denoted $\tilde{\Omega}$ and the physical frequency Ω is given by

$$\Omega = \left[\frac{\Upsilon y}{8x\gamma}\right]^{1/2} \tilde{\Omega} \equiv \kappa\tilde{\Omega}, \quad \kappa \equiv \left[\frac{\Upsilon y}{8x\gamma}\right]^{1/2} \tag{82}$$

where y is the density of libration modes per unit volume in the material, and $\gamma = \mu/\tilde{\mu}$ is the high-frequency shear modulus divided by the value used in the computer. If we make a change of variables to $\tilde{\Omega}$ in (28), we get

$$B = B'(\omega=0) = \frac{8x}{\tilde{\mu}} \int d\tilde{\Omega} \frac{\tilde{p}(\tilde{\Omega}) A_b^2}{\tilde{\Omega}^2} , \tag{83}$$

where $\tilde{p}(\tilde{\Omega}) = \kappa p(\Omega)/y$ is the normalized density of defect states in the simulation. Note that everything in this equation only depends on numbers taken out of the computer, so the amount of softening can be determined without knowing the magnitude of the physical elastic constants.

It is interesting that the change in elastic constants given in Eq. (83) is independent of both the concentration of dipoles y, and of the defect parameter $\Upsilon = Q_0^2/I$. The reason is slightly different in the two cases, although in both of them it is because the change in elastic constants due to a libration mode is proportional to $1/\Omega^2$. B is independent of y because the interaction dies off like $1/r^3$. If we double y, we have twice as many modes, but the modes have frequencies that are $\sqrt{2}$ times higher. Since the change in elastic constants is like $1/\Omega^2$, these effects cancel. Estimating in a simple way the effect of changing x gives the same result, although here we will not be exactly right, since presumably changing x changes the shape of $f(\tilde{\Omega})$ as well as its peak frequency. The reason that Υ has no effect on B is mathematically the same—B increases linearly with Υ—but the frequencies of the libration modes increase like $\sqrt{\Upsilon}$, and again, the effects cancel. This discussion is only true, of course, when we can neglect the effect of the "local field" on the dipoles, as we have in our model. In KBr:KCN, for example, as we lower the concentration of cyanides, at some point the local field will become more important than the interaction between cyanides, and we would expect B to decrease linearly with concentration below this point.

B. "Local-field" effects

The basic reason why we obtain the "universal" results given above within our model is the following. The interaction between defects is mediated by the phonons. Thus the frequency scale of the defect modes is determined by the *same* coupling constant Υ that determines the phonon scattering. This leads to independence of Υ. The $1/r^3$ nature of the interaction is responsible for the concentration independence.

Although this universality is an appealing feature of the elastic dipole model, we now investigate to what extent the assumptions that give rise to it are valid for real glasses. (For a discussion motivating this model for glasses, the reader is referred to Sec. II of I.)

The $1/r^3$ dependence is crucially dependent on the defects being elastic dipoles, and not having any higher multipoles associated with them. However, our basic picture, that resonant scattering from localized harmonic modes causes the plateau, can surely be true without the $1/r^3$ interaction being crucial. We have run a simulation (with the model parameters of KBr:KCN) with second-rank traceless symmetric tensors interacting via near-neighbor interactions, and we still find a plateau in the thermal conductivity.

The universality with respect to the defect parameter Υ hinges on the neglect of "local-field" effects. As we had emphasized while introducing the elastic dipole model (see Sec. II of I), this is one of the simplest models within which to study the low-temperature properties of glasses. Since thermal transport requires the defect-phonon coupling, there is no way to "turn off" the phonon-mediated interaction between defects. In the glassy phase of KBr:KCN we know that the local-field effects are small (see Sec. IX), but, in general, we have no arguments other than simplicity to rule out the importance of these effects. Our results show that local-field effects are certainly not necessary to explain the plateau.

For a high enough concentration of defects, it is not unreasonable to believe that the interactions dominate over the effect of the local environment. At low concentrations we certainly expect these arguments to break down, as discussed above for the softening. We would then expect the scattering to get less important, since as the concentration decreases, the frequency will not decrease to compensate, and will be fixed at a value determined by the local field.

One check on this argument is that as the concentration of defects is increased in a crystal, one expects first to not have a plateau, and then for the plateau to become prominent first at low temperature, and then move to higher temperatures as the concentration is increased. In the regime where the local fields are negligible, the temperature of the plateau should scale like $\sqrt{x}$. Both of these observations seem to be true[5] in $(KBr)_{1-x}(KCN)_x$.

In general, of course, it is difficult to take a crystal and adjust the concentration of defects. One system where this can possibly be done is neutron-irradiated quartz.[36] Here, the scenario sketched above does not hold as well. Initially, as the dose of neutrons is turned up, the thermal conductivity just drops, and a plateau does not appear at low temperatures. This could be due to strong local fields in the system. Clearly, in this system an isolated defect is not free to rotate, as it is in our model. At the highest doses the plateau moves to somewhat higher temperature, but the effect is rather small.

Finally, let us discuss the fits of the thermal properties of the elastic dipole model of vitreous silica. There are two features in our phenomenological fits which should be mentioned. First, the fit to the neutron density of states gave a value for $\Upsilon = Q_0^2/I$ that is an order of magnitude larger than the corresponding value for KBr:KCN. Since we have no microscopic picture for what the "defects" are in a-SiO_2, it is difficult to say if this is "reasonable" or not. Nevertheless, the following crude estimates may be of some interest. In KBr:KCN the dipole moment $Q_0 \sim 1$ eV. Since the elastic constants of silica are an order of magnitude stiffer than that of KBr:KCN, and $Q_0 \propto \mu$, we would expect, assuming that the "defects" are the same "shape," that Q_0 for silica would be roughly an order of magnitude larger. (This is much higher than the characteristic 1-eV coupling to the TLS in glasses; however, it must be kept in mind that the TLS are rare and could well have atypical phonon couplings.) On the other hand, if we envision our defects as rotating SiO_4 tetrahedra or as flopping oxygens, the moment of inertia I will probably be considerably larger than that of a cyanide molecule in KBr. Given this picture, a value of $\Upsilon = Q_0^2/I$ which is 10 times that for KBr:KCN could be possible.

Second, although we match the low-frequency phonon density of states of silica, we are not able to match the two elastic constants λ and μ individually. The elastic dipole model leads to too soft a shear modulus, i.e., too small a renormalized λ/μ for almost any reasonable[37] bare λ/μ. Adding a local field (due to the "cage" in which the defect "sits") to our model could solve this

problem by preventing the softening of the shear modulus. This would also give rise to a larger libration frequency with a smaller value of Υ.

IX. APPROXIMATIONS, STRENGTHS, AND WEAKNESSES

The model that we have been analyzing—randomly placed elastic dipole in an elastic medium—is a strongly interacting random system, and in order to make any progress it was necessary to make several simplifying assumptions and approximations, some of which might be left buried in the middle of the calculation. In a paper this long, with a mix of analytical and numerical computations, many interested readers will not work through the details of our calculations. We believe that it is therefore especially important to critically discuss at one place all of the approximations that we have made and assess the strengths and weaknesses of our approach. This is in itself a strength: our theory is sufficiently quantitative that we can identify all of the simplifications and approximations separating our results from the real world.

We will divide the discussion into two broad categories: (a) assumptions built into the model from the start, and (b) approximations made in the process of analyzing the model.

For a detailed discussion of the elastic dipole model we refer the reader to Sec. II of I. We first discuss our use of elasticity theory. The use of linear-elasticity theory down to interatomic distances is itself an approximation. We assume that the "defects" can be characterized as point defects, and we only include the lowest nontrivial (elastic dipole) term in the multipole series for elastic defects. We then assume a particular form for the elastic dipole (traceless, axially symmetric), and take all dipoles to be identical. We neglect electrostatic interactions (electric-dipole–dipole, etc.). These approximations are well justified for KBr:KCN. For a general glass this scheme of considering isolated point defects embedded in a continuum is justified only on grounds of simplicity. Relaxing these approximations would probably not give strikingly different behavior, but would increase the number of free parameters.

We further assume that the dynamics of the "defects" is completely dominated by the interactions between defects mediated by the strain field. As emphasized earlier, since one has a strong phonon-defect coupling in glasses, and a large concentration of defects, it would appear unreasonable to ignore the interaction between defects. What is not *a priori* obvious is the neglect of local fields, i.e., the assumption that a single isolated defect has no preferred orientation. The neglect of local fields, in addition to reducing the number of free parameters, has an important consequence. As discussed at length in Sec. VIII of this paper, it leads to the existence of a plateau independent of the parameters of our model. If local fields were important, we would lose this universality. However, whether local fields are important or not is an experimental question.

For $(KBr)_{1-x}(KCN)_x$, neglecting the crystal fields is justified experimentally; for the range of x where glassy behavior is seen, the local field (of about 5 K) is much smaller than the energy scale of interactions (hundreds of degrees Kelvin). Furthermore, within this approximation we obtain reasonably good agreement for the low-frequency softening of the material due to the dipole degrees of freedom [comparing $(KBr)_{0.5}(KCN)_{0.5}$ with KBr]. As shown in Sec. VII, we can obtain the thermal-conductivity plateau for a-SiO_2 from our model which ignores local-field effects. However, as discussed at the end of Sec. VIII, these effects might, in fact, be important for getting the right elastic properties.

We next turn to the various approximations we make in analyzing the elastic dipole model. At the very outset we make a conceptual separation between the interacting defect system and the long-wavelength phonon modes of the elastic medium. We should emphasize that it is only through a combined use of numerical and analytical techniques that we are able to study, e.g., the thermal transport in our model: a numerical study of the normal modes of the defect system, followed by a perturbative treatment of the interaction of the libration modes with the low-frequency phonons. A purely numerical treatment might allow a study of the true normal modes of the system, which mix the defect libration and phonon degrees of freedom. However, due to finite-size effects it would be impossible to include long-wavelength phonons and thus an analysis of the thermal conductivity would be limited to rather high temperatures (see, e.g., Ref. 38).

Let us now examine some of the approximations involved in more detail. First, in calculating the effective Hamiltonian for the interacting defect dipoles, we "integrate out" the phonon degrees of freedom assuming that the phonons relax instantaneously on the time scale of the defect dynamics; see Sec. III of I. The validity of this approximation is not *a priori* clear since it depends on the values of the parameters. As shown in Sec. VII of this paper, for KBr:KCN this approximation is only moderately well justified; for vitreous silica the separation of time scales between the libration modes and the Debye-frequency phonons is reasonably large.

After the defect Hamiltonian has been derived, the simulation is straightforward, as described in Sec. IV of I. We obtain the harmonic excitations about the disordered ground states of the simulation by numerically diagonalizing the dynamical matrix; see Sec. II. We verify that the anharmonicity of these coupled angular oscillation modes—the librations—is rather small, and also that the density of states for these modes is extremely insensitive to the system size. However, finite-size effects prevent us from determining directly whether the libration modes are localized or not. We assume that the libration modes do not contribute significantly to thermal transport.

We take the coupling between the disordered libration modes and low-frequency phonons to be bilinear, thus obtaining a random harmonic system. In calculating the coupling between libration modes obtained in the simulation and the long-wavelength phonons, we use the approximation that we may effectively set the phonon wave vector $\mathbf{k} \to \mathbf{0}$. This is certainly justified for sufficiently long-wavelength phonons if the libration modes are local-

ized. But even if they are not localized, the librations bear little resemblance to plane waves, and their coupling to phonons is expected to be qualitatively unchanged by including spatial modulation of the phonon amplitude.

The resonant scattering rate of phonons from the libration modes is so large that $\omega\tau \sim O(1)$ near the peak in the libration density of states. Our lowest-order perturbation theory result might seem to be inadequate in this regime. However, we have shown[7] that a simple estimate of the higher-order terms, which could give rise to phonon localization in a narrow band, does not affect the final result for the thermal conductivity. Since thermal conductivity is a broadband measurement, it is insensitive to whether phonons in a narrow range of frequencies are strongly scattered or localized; see Ref. 7.

It is not equally clear if the perturbative analysis of the effect of the phonon-libration coupling on the total density of harmonic excitations (needed for the excess specific heat) is insensitive to higher-order corrections. In general, the C/T^3 curves are quite sensitive to details of the density of states, unlike the thermal-conductivity plateau.

Once the scattering rate from the libration modes has been calculated, the thermal-conductivity computation proceeds along a standard route. The approximations involved—use of the Boltzmann equation within a relaxation-time approximation, Matthiesen's rule for adding the rates due to various mechanisms, etc.—are well known, and so we will not comment upon them further.

X. RELATION TO OTHER THEORIES

In this paper and its companion (I) we have introduced and analyzed the elastic dipole model to understand the low-temperature properties of glasses. In I we numerically studied the frozen ground states of this model, and thermally activated excitations which involve a reorientation of the dipoles. There we compared our results with two analytical approaches to study these excitations in other models of "quadrupolar" glasses (see Sec. VI of I). We also compared our work with various microscopic models for mixed alkali-halide–alkali-cyanide systems (see Sec. VIII of I). In this section we will attempt a broader discussion comparing our work with other theories of low-temperature properties of glasses.

We must first address the obvious question: Is our model a glass? It is not formed by quenching an equilibrium liquid into a frozen configuration: the lattice disorder is frozen in at a temperature high compared to the orientational freezing temperature. For studying the glass transition, our model is more closely related to spin glasses than to window glass.

However, it is becoming increasingly clear that the low-temperature thermal and elastic properties of glasses are not uniquely dependent upon the way glasses are formed. Several glassy crystals have low-temperature specific heats, thermal conductivities, elastic properties, and dielectric losses which are indistinguishable from those found in more traditional covalent, polymer, and molecular glasses. We have a successful numerical model of one of these glassy crystals, $(KBr)_{1-x}(KCN)_x$. While our model is surely not applicable in detail to all glasses, a general theory of the low-temperature properties of glasses should make sense in the context of our model and KBr:KCN. It is rather implausible that exactly the same behavior will occur in glasses and glassy crystals for completely different reasons. As we have shown above, if we fix the parameters for the elastic dipole model from neutron-scattering measurements on silica, without asking for a detailed microscopic picture, our model is able to account for the thermal conductivity plateau in a-SiO_2.

In this paper we have only applied our model to the intermediate-temperature properties, and simply assumed the existence of tunneling centers or the TLS which account for the very low-temperature properties. For KBr:KCN it has been suggested[39] that 180° reorientations of isolated cyanides comprise the tunneling degree of freedom in the TLS model. Extrapolating the distribution of barriers measured in dielectric loss to very low barrier heights leads to about the right number of active tunneling centers necessary for the low-temperature specific heat; see Ref. 40. However, it should be noted that in a similar material, $CO/N_2/Ar$, it has been seen experimentally[41] that the low-temperature specific heat is unchanged as the symmetric molecule N_2 is substituted for the asymmetric molecule CO. This indicates that the excitation responsible for at least the low-temperature specific heat in $CO/N_2/Ar$ is more complicated than the simple reorientation of the diatomic molecule.

It would conceivably be possible to look for tunneling centers, whether or not they are more complicated than simple 180° reorientations of the defects, in the elastic dipole model, and to extend the analysis to include the very-low-temperature behavior. This is difficult for several reasons. One is that the true tunneling centers are presumably very rare. In glasses typically only about 1 in 10^5 atoms or so is able to quantum-mechanically tunnel on experimental time scales. The other difficulty is that the structure of the energy surface is very complicated; even for a small number of dipoles there are many local minima. Despite the possible difficulty, we think that elucidating the nature of the low-energy states is a very interesting area for future work.

Let us now turn to the main subject of this paper—the intermediate-temperature properties of glasses. There are several early theories that we can rule out for KBr:KCN using our model. For structural glasses, also, these proposals do not appear to be viable for reasons given below.

Two previous theories exist for the anomalous contribution to the specific heat. The first[42] attributes it to a hierarchy of tunneling centers with new tunneling centers relaxing only after others move. The second[43] uses the detailed dipole-dipole form of the interactions between pairs of centers to predict a crossover of the specific heat from linear to cubic in temperature. We find that the anomalous specific heat in our model is due to harmonic excitations, and not due to collective effects involving the tunneling degrees of freedom. In addition, there is experimental evidence[1] that the excess specific heat is time independent, and thus qualitatively different from the low-temperature linear term. Also, as mentioned earlier, in vitreous silica Buchenau *et al.*[10] have made a direct connection between harmonic excitations and the anomalous specific heat.

There have been several recent suggestions linking the plateau in the thermal conductivity with localization of short-wavelength normal modes in amorphous materials either due to strong scattering from structural disorder,[27] or due to the postulated fractal nature[44] of glasses. All these approaches need to introduce a new characteristic length scale which is roughly 10 times the lattice spacing.

The first[27] attributes the plateau to Rayleigh scattering from density or coupling-constant fluctuations. This picture was motivated by using the dominant phonon approximation to extract a mean free path l which, as we have discussed above (at the end of Sec. VI), is not valid in the plateau regime. Further, a quantitative estimate of the Rayleigh scattering in KBr:KCN, and even in structural glasses,[26] is far too small to explain the plateau. Finally, as shown in Ref. 7, the only way to get strong scattering ($\omega\tau = kl \sim 1$) from structural disorder is to have the phonon wavelength k^{-1} match the scale R_0 on which the disorder occurs, i.e., $kR_0 \sim 1$. We do not believe that there is any independent evidence for, say, density fluctuations, on a length scale comparable to the thermal phonon wavelength in the plateau regime.

The fracton theory[44] postulates that amorphous materials are self-similar below this correlation length, an assumption for which there is little direct evidence in bulk glasses. Then the harmonic, localized, vibration modes of the fractal structure, called fractons, lead to the plateau. While resonant scattering off of rather localized modes is important in our picture, we see no evidence that our libration modes are dynamically fractal. We believe that direct experimental evidence for the fractal nature of bulk glasses will be necessary for this theory to gain more general acceptance.

There are several recent theories[8,9] which also relate the specific heat and the plateau to extra localized vibration modes, as we do. While the details of our analysis and of our results are clearly rather different, we share the same general picture.

The first, due to Karpov and Parshin,[8] beings with an explicit model of a double well written as a quartic polynomial in some configurational coordinate. Within the parameter space of all such potentials, they also have degrees of freedom with positive quadratic terms, i.e., single wells; the double wells are responsible for the TLS. These authors suggest that resonant scattering from the single-well modes is responsible for the plateau, but no quantitative estimates are provided. An issue on which we disagree is the rise in the thermal conductivity above the plateau. Karpov and Parshin suggest that this is due to the resonant scattering of low-frequency phonons from TLS, but as we have shown in Ref. 7 this effect is masked by other scattering mechanisms. The rise, above the plateau, in our model is related to the drop in the libration DOS, and it is Rayleigh scattering which dominates above the plateau. Finally, our libration modes are small oscillations of the elastic dipoles within one of the double wells, rather than in their single wells.

The second proposal, due to Yu and Freeman,[9] attempts to fit the plateau and the anomalous specific heat with an assumed step-function density of states of additional localized harmonic modes. These authors were unable to fit both with a single set of parameters. In addition, Yu and Freeman needed to include a large amount of Rayleigh scattering to fit the plateau. As discussed above, the detailed positions and magnitudes of the plateau and the bump in the specific heat are highly sensitive to the form of the onset of the additional modes. The assumed onset in Ref. 9 is presumably too abrupt. Indeed, our original simpler attempts[7] found much too large a bump in C/T^3 as well. The numerical results presented here demonstrate that additional modes suffice to explain both the plateau and the anomalous specific heat in KBr:KCN and in vitreous silica, without the need to invoke enhanced Rayleigh scattering.

It may be of interest to note that recent computer simulations[45] of glasses have identified localized vibrational modes in amorphous silicon. Such modes should be a ubiquitous feature of glasses from the point of view of our model.

Finally, we must discuss the ongoing theoretical work by Yu and Leggett.[21] They argue that the traditional tunneling center or TLS theory of glasses below 1 K is incomplete or wrong, and that a proper understanding of these very-low-temperature properties will also lead to an understanding of the intermediate-temperature properties (the subject of this paper). While their analysis is still incomplete, their initial formulation shares several features with our model. First, they argue that the important degrees of freedom are stress sources with $1/r^3$ interactions, a specific example of which would be our elastic dipole defects. Second, they argue as we do that the interactions between these degrees of freedom dominate the physics, in contrast to the noninteracting TLS, whose properties are determined from their local environments. Third, the $1/r^3$ asymptotic form of the interactions is crucial for the scaling arguments of Ref. 21. The argument for the universality of the plateau in our model independent of the density of defects, presented in Sec. VIII, also relies on the $1/r^3$ form of the interaction.

On the other hand, there are several features of our treatment which clearly differ from the Yu-Leggett approach. First, in some early simulations we tried using nearest-neighbor interactions between the dipoles. We observed roughly the same behavior at $x=0.5$ in both the specific heat and the thermal conductivity as in the $1/r^3$ simulations. Their argument for the plateau appears to rest firmly on the $1/r^3$ form of the interaction. While we agree that for the plateau to be independent of dipole concentration requires a $1/r^3$ interaction, the plateau exists at high concentrations of dipoles without long-range couplings. Second, our basic views on the origin of these intermediate-temperature properties differ. In their picture, the plateau is a crossover phenomenon, when the phonon frequency $\hbar v/\lambda$ (where v is the speed of sound and λ the wavelength) matches the interaction energy between dipoles separated by λ. This is the point where the time-related nature of the interaction makes the static elastic dipole potential break down. (Perversely, the static interaction in their approach works best for the *low*-frequency phonons, because the interactions they mediate are at even lower energies.) In our model, the plateau occurs when the frequency scale of the phonons matches

that of the libration modes. We have ignored the time-retarded nature of the interaction in calculating the frequencies of the libration modes, but this appears to be a reasonable first approximation: more so for the parameters relevant to silica than for KRr:KCN.

We share with Yu and Leggett a dissatisfaction with the traditional tunneling-center approaches. We do believe, however, that quantum tunneling is probably necessary to get the very long time scales and the large density of states at low energies. Low-energy excitations at long wavelengths should be suppressed by phase space; also, they ought to contribute to thermal transport (which experimentally is dominated by phonons[46]). The only way we can see to have localized low-energy excitations involves tunneling through barriers. We believe also that more or less localized harmonic excitations are responsible for the plateau and the anomalous specific heat at intermediate temperatures in glasses.

XI. CONCLUSIONS

In this paper and its companion (I) we have introduced a simple model—the elastic dipole model—and shown that it is able to provide a natural explanation for the universal intermediate-temperature properties of glasses. We conclude by summarizing the basic physical picture that emerges from the calculations reported above. We have studied the harmonic excitations about the disordered ground states of the elastic dipole model. The "additional" harmonic excitations, the librations, of our model have a strongly peaked density of states. The coupling of these modes to the long-wavelength phonons leads to a softening of the shear modulus of the elastic medium, but has no effect on the bulk modulus. This is due to the relaxation of the dipoles in the presence of an externally applied stress. The libration density of states accounts for the excess specific heat seen as a bump in C/T^3. Phonons in the plateau region are on resonance with the libration modes and are thus very strongly scattered. This gives rise to a plateau in the thermal conductivity.

ACKNOWLEDGMENTS

We are pleased to thank Andy Anderson, Ulrich Buchenau, Dave Cahill, Hank Fischer, Tony Leggett, Bobby Pohl, Susan Watson, and Clare Yu for discussions on the low-temperature properties of glasses. We gratefully acknowledge support by U.S. National Science Foundation (NSF) Grant No. DMR-82-17227-A01 through the Materials Science Center at Cornell University, and by NSF Grant No. DMR-86-12860 at the University of Illinois. One of us (E.R.G.) was partially supported by the NSF. We also acknowledge use of the Cornell National Supercomputer Facility, a resource of the Center for Theory and Simulation in Science and Engineering at Cornell University, which is funded in part by the NSF, the State of New York, and the IBM Corporation.

APPENDIX: REAL NUMBERS

Here we describe the procedure by which we go from the numbers which come out of the simulation to physical units. We will denote the units used in the simulation by placing a tilde over the corresponding physical unit. So if the volume of a physical unit cell is r^3, then the volume of the unit cell in the simulation is $\tilde{r}^3$. Similarly, for the elastic constants, if μ is the physical high-frequency shear modulus, then $\tilde{\mu}$ would be the value used in the simulation. For a given configuration, the energy in the simulation is calculated by Eq. (1),

$$H=-\tfrac{1}{2}\sum_{\substack{\mathbf{x},\mathbf{r}'\\(\mathbf{x}\neq\mathbf{r}')}} Q_{ij}(\mathbf{r}')J_{ijkl}(\mathbf{x}-\mathbf{x}')Q_{kl}(\mathbf{x}') \ . \tag{A1}$$

In general, J_{ijkl} has units of

$$\frac{1}{(\text{elastic constant})\times(\text{volume})} \ , \tag{A2}$$

so to go from the energy in the computer to a physical energy, we have the following conversion,

$$E=Q_0^2(\tilde{c}/c)(\tilde{r}/r)^3\tilde{E} \ , \tag{A3}$$

where $\tilde{c}$ is one of the computer elastic constants, and c is the corresponding physical elastic constant. We must multiply by Q_0^2 since we have set Q_0 equal to 1 in the simulation. Note that since $\tilde{r}$, $\tilde{c}$, and the other computer values are unitless, the units are correct.

We define $\gamma\equiv\mu/\tilde{\mu}$. To go from computer units to real units, we need to know γ and $\tilde{r}/r$. At this point we do not know what the value of γ is, since we do not know the high-frequency "bare" value of μ, only the low-frequency measured value.

On the other hand, we can obtain a value for $\tilde{r}/r$ by knowing y, the density of modes per unit volume in the real material. In the simulation we have put dipoles on fraction x of the sites of a fcc lattice. We want to know the "real" length of a side of a conventional unit cell, which the computer thinks is one unit long. Of course, in KBr:KCN we know the size of the unit cell, but since we want to apply our model to glasses in which the defects are not on a fcc lattice, we will need to determine this length by matching the density of defect modes. For $x=0.5$ there are four dipoles per unit cell and two modes per dipole; thus we have

$$8x\tilde{r}^3=yr^3 \Longrightarrow (\tilde{r}/r)^3=(y/8x) \ . \tag{A4}$$

The energy conversion is then given by

$$E=\frac{Q_0^2 y}{8x\gamma}\tilde{E} \ . \tag{A5}$$

The frequency of a normal mode, Ω, is determined from $\tilde{\Omega}$, the square root of an eigenvalue of the dynamical matrix, by

$$\Omega=\left[\frac{\Upsilon y}{8x\gamma}\right]^{1/2}\tilde{\Omega}\equiv\kappa\tilde{\Omega} \ , \tag{A6}$$

defining κ. From the simulation, we can calculate $\tilde{p}(\tilde{\Omega})$, the distribution of $\tilde{\Omega}$, which we have normalized,

$\int d\tilde{\Omega}\,\tilde{p}(\tilde{\Omega})=1$. The density of libration mode states per unit volume in the real material, $p(\Omega)$, is then given by

$$p(\Omega)=(y/\kappa)\tilde{p}(\Omega/\kappa)\ . \tag{A7}$$

We now calculate the change in the elastic constants due to this density of states. At zero frequency recall that the change in elastic constants is determined by

$$B=\frac{8x}{\tilde{\mu}}\int d\tilde{\Omega}\,\frac{\tilde{p}(\tilde{\Omega})\overline{A^2}}{\tilde{\Omega}^2}\ . \tag{A8}$$

Using Eq. (55) for the mean speed of sound in an isotropic material, and (29) for the softened elastic constants, we find the low-frequency Debye velocity,

$$v_D=\left[\frac{\gamma\tilde{\mu}}{\rho(1+B/5)}\right]^{1/2}\left[\frac{3}{2+\{\tilde{\mu}/[\tilde{\lambda}+2\tilde{\mu}+(B/5)(\frac{2}{3}\tilde{\mu}+\tilde{\lambda})]\}^{3/2}}\right]^{1/3}\ . \tag{A9}$$

This gives

$$\gamma=\frac{v_D^2\rho(1+B/5)}{\tilde{\mu}}\left[\frac{2}{3}+\frac{1}{3}\left[\frac{\tilde{\mu}}{[\tilde{\lambda}+2\tilde{\mu}+(B/5)(\frac{2}{3}\tilde{\mu}+\tilde{\lambda})]}\right]^{3/2}\right]^{2/3}\ . \tag{A10}$$

Now we know γ in terms of the measured Debye velocity and the inputs to the simulation, x, $\tilde{\mu}$, and $\tilde{\lambda}$. As we have mentioned before, only the ratio of $\tilde{\mu}$ and $\tilde{\lambda}$ is important, if we double $\tilde{\mu}$ and $\tilde{\lambda}$, this lowers the computer's energy scale, so that B also doubles, and finally γ will end up being halved, giving the same high-frequency values for μ and λ, as desired. Now that we know the "bare" values of μ and λ, we know everything we need to know, since we will take Υ and y from experiment.

*Present address: AT&T Bell Laboratories, 600 Mountain Avenue, Murray Hill, NJ 07974-2070.

†Permanent address: Department of Physics, State University of New York, Stony Brook, NY 11794-3800.

[1]S. Hunklinger and A. K. Raychaudhari, in *Progress in Low Temperature Physics IX,* edited by D. F. Brewer (Elsevier, New York, 1986), p. 265.

[2]*Amorphous Solids, Low Temperature Properties,* edited by W. A. Phillips (Springer-Verlag, Berlin, 1981).

[3]P. W. Anderson, B. I. Halperin, and C. M. Varma, Philos. Mag. **25**, 1 (1972); W. A. Phillips, J. Low Temp. Phys. **7**, 351 (1972).

[4]R. C. Zeller and R. O. Pohl, Phys. Rev. B **4**, 2029 (1971).

[5]J. J. De Yoreo, W. Knaak, M. Meissner, and R. O. Pohl, Phys. Rev. B **34**, 8828 (1986), and references therein.

[6]E. R. Grannan, M. Randeria, and J. P. Sethna, Phys. Rev. Lett. **60**, 1402 (1988).

[7]M. Randeria and J. P. Sethna, Phys. Rev. B **38**, 12 607 (1988); M. Randeria, Ph.D. thesis, Cornell University, Ithaca, NY, 1987 (unpublished).

[8]V. G. Karpov and D. A. Parshin, Zh. Eksp. Teor. Fiz. **88**, 2212 (1985) [Sov. Phys.—JETP **61**, 1308 (1985)].

[9]C. C. Yu and J. J. Freeman, Phys. Rev. B **36**, 7620 (1987).

[10]U. Buchenau, M. Prager, M. Nucker, A. J. Dianoux, N. Ahmad, and W. A. Phillips, Phys. Rev. B **34**, 5665 (1986); U. Buchenau, H. M. Zhou, N. Nucker, K. S. Gilroy, and W. A. Phillips, Phys. Rev. Lett. **60**, 1318 (1988). See also U. Buchenau, N. Nucker, and A. J. Dianoux, *ibid.* **53**, 2316 (1984).

[11]E. R. Grannan, M. Randeria, J. P. Sethna, this issue, the preceding paper, Phys. Rev. B **41**, 7778 (1990).

[12]For simplicity we take the phonon density of states to be of the Debye form, i.e., ω^2 up to a cutoff ω_D. Neglecting the dispersion of the *bare* phonons (that is, before including the interactions with the defect modes) has no qualitative effect on our results.

[13]E. R. Grannan, Ph.D. thesis, Cornell University, Ithaca, NY, 1989.

[14]Obtaining this result from considerations of the elastic-constant tensor, rather than the compliance tensor, is possible, but a little more tricky. This analysis proceeds from applying an external *strain* field. However, it must be remembered that the *total* uniform strain field has contributions from both the externally applied one and the induced response of the dipole defects.

[15]An upper bound on μ and K is obtained from the Voigt average, which is a spherical average of the elastic-constant tensor; the Reuss average of the compliance tensor provides a lower bound. See J. P. Hirth and J. Lothe, *Theory of Dislocations* (Wiley, New York, 1968), p. 399.

[16]For $x=0.7$ the orientations of the dipoles are correlated over the size of the system and point preferentially in the $\langle 111\rangle$ directions, as discussed in I. This leads to a marked cubic component to the elastic constants, and the two methods of spherical averaging give λ/μ values which differ by order unity.

[17]Note that in our earlier work (Ref. 6) we had found $\overline{A^2(\Omega)}$, which was a very weak function of Ω, in contrast to the result found here. This difference is due to the inclusion of the uniform $\mathbf{k}=\mathbf{0}$ strain mode in the defect Hamiltonian (see I), which enhances the tendency for the frozen dipoles to be aligned and gives rise to low-frequency librations which couple rather strongly with the phonons. Since $\overline{A^2(\Omega)}$ always appears multiplied with the strongly peaked libration DOS, $p(\Omega)$, we will find that its frequency dependence does not have a major effect on the final results.

[18]In Ref. 6 we had used the corresponding equations which are valid to only *first order* in B. To this order, the changes in λ and μ are given by $\mu(0)\sim\mu(1-B/5)$ and $\lambda(0)\sim\lambda+(2B/15)\mu$, but, as it turns out, the changes in λ and μ are

not small, being of the order of the elastic constants themselves.

[19]D. L. Huber and J. H. Van Vleck, Rev. Mod. Phys. **38**, 187 (1966).

[20]The real part of the shift $\Delta(\omega)$ is of the form

$$\Delta(\omega)\sim\frac{\Upsilon A_b^2}{\rho}\mathrm{P}\int d\omega_k\frac{\omega_k^4}{\pi^2 v^5(\omega^2-\omega_k^2)}\ .$$

This is essentially a negative constant independent of ω, for $\omega\ll\omega_{\mathrm{Debye}}$, since the integral above is dominated by frequencies near the Debye frequency. Δ can be interpreted as a shift in the frequency of the libration mode due to a renormalization of the moment of inertia I. Since we use the effective moment of inertia for a defect embedded in the host lattice, the density of states that we obtain from our simulation is already in terms of the renormalized frequencies.

[21]C. C. Yu and A. J. Leggett, Comm. Condens. Mater. Phys. **14**, 231 (1988).

[22]A. C. Anderson, in *Amorphous Solids, Low Temperature Properties* (Ref. 2).

[23]D. P. Jones and W. A. Phillips, Phys. Rev. B **27**, 3891 (1983).

[24]J. Jäckle, Z. Phys. **257**, 212 (1972).

[25]S. Hunklinger and W. Arnold, in *Physical Acoustics,* edited by R. N. Thurston and W. P. Mason (Academic, New York, 1976), Vol. 12.

[26]See Refs. 46 and 23. Also see: J. Jäckle, in *The Physics of Non-Crystalline Solids,* edited by G. H. Frischat (Trans Tech, Rockport, MA, 1977), p. 568.

[27]J. E. Graebner, B. Golding, and L. C. Allen, Phys. Rev. B **34**, 5696 (1986).

[28]Recent measurements (see Ref. 47) of the cyanide concentrations of the $(KBr)_{1-x}(KCN)_x$ samples used by De Yoreo *et al.* indicate that the actual concentrations of the samples were $x=0.19$, 0.41, and 0.60. We will neglect this and compare to the nominal values of 0.25, 0.5, and 0.7.

[29]A. S. Nowick and W. R. Heller, Adv. Phys. **12**, 251 (1963).

[30]H. Beyeler, Phys. Rev. B **11**, 3078 (1975).

[31]R. Spitzer, Ph.D thesis, Cornell University, Ithaca, NY, 1987.

[32]Since the coupled random Hamiltonian for the phonons and librations is quadratic, in principle we could discuss localization by diagonalizing it and finding its true normal modes. As argued in Ref. 7, our perturbative calculation simply estimates possible mobility edges for the true normal modes.

[33]W. Dietsche and H. Kinder, Phys. Rev. Lett. **43**, 1413 (1979).

[34]W. Dietsche (private communication).

[35]One way in which this argument could fail to give a plateau would be if the scattering from this method was masked by some other form of scattering. For example, if the energy scale of the libration modes was large enough, Rayleigh scattering would become important before the thermal phonons were in resonance with the libration modes.

[36]A. M. de Goër, in *Phonon Scattering in Condensed Matter V,* edited by A. C. Anderson and J. P. Wolfe (Springer-Verlag, Berlin, 1986).

[37]To get the correct low-frequency elastic constants in silica, we need a bare (high-frequency) $\lambda<0$. While the bare bulk modulus K is positive, so that thermodynamic stability is not violated, this is rather unusual.

[38]P. B. Allen and J. L. Feldman, Phys. Rev. Lett. **62**, 645 (1989).

[39]J. P. Sethna and K. S. Chow, Phase Trans. **5**, 317 (1985); J. P. Sethna, Ann. N.Y. Acad. Sci. **484**, 130 (1986).

[40]L. Wu, R. M. Ernst, Y. H. Jeong, S. R. Nagel, and S. Susman, Phys. Rev. B **37**, 10 444 (1988).

[41]C. I. Nicholls, L. N. Yadon, D. G. Haase, and M. S. Conradi, Phys. Rev. Lett. **59**, 1317 (1987).

[42]C. M. Varma, R. C. Dynes, and J. R. Banavar, J. Phys. C **15**, 1221 (1982).

[43]M. W. Klein, Phys. Rev. B **29**, 5825 (1984).

[44]S. Alexander *et al.*, Phys. Rev. B **28**, 4615 (1983); S. Alexander, O. Entin-Wohlman, and R. Orbach, *ibid.* **34**, 2726 (1986).

[45]R. Biswas, A. M. Bouchard, W. A. Kamitakahara, G. S. Grest, and C. M. Soukoulis, Phys. Rev. Lett. **60**, 2280 (1988).

[46]M. P. Zaitlin and A. C. Anderson, Phys. Rev. B **12**, 4475 (1975).

[47]S. K. Watson, D. G. Cahill, and R. O. Pohl, Phys. Rev. B **40**, 6381 (1989).